Physics – Uspekhi **38** (9) 965 – 990 (1995)

PACS numbers: 43.25.+y

Nonlinear sawtooth-shaped waves

O V Rudenko

Contents

Abstract. This survey is devoted to experimental and theoretical results on interaction and self-action processes of strongly distorted waves containing shock fronts. Such sawtooth-shaped disturbances can be formed during the propagation of the wave through media where the nonlinearity predominates over competitive factors like dispersion, diffraction and absorption. The specificity of nonlinear processes for sawtooth-shaped waves is particularly emphasised. The recently observed phenomena such as self-action of beams, self-refraction of shock pulses and saturation of the signal in focus, as well as current applied problems, are described.

1. Introduction

The sawtooth-shaped wave is an unconventional and interesting subject of investigation which can be experimentally observed in distributed systems of diverse physical nature. A rich variety of experimental data on the nonlinear dynamics of sawtooth-shaped waves has been obtained in nonlinear acoustics. That is why it is convenient to discuss most of the nonlinear phenomena associated with the propagation and interaction of such waves using the example of a high-intensity acoustic wave.

O V Rudenko Physics Department, M V Lomonosov Moscow State University, Vorob'evy gory, 119899 Moscow, Russia
Tel. (7-095) 939 29 36
E-mail: rudenko@na.phys.msu.su

Received 23 February 1995, revised 20 March 1995
Uspekhi Fizicheskikh Nauk **165** (9) 1011 – 1036 (1995)
Submitted in English by the author; edited by H Milligan

Nonlinear acoustics is often referred to not only as the modern division of acoustics, but also as a principal part of nonlinear wave physics. The dispersion of sound velocity is very weak in acoustic media, and wave interactions have many distinctive properties under these conditions. It is agreed that in many problems of nonlinear acoustics the dispersion is absent altogether. In this situation, essentially all virtual processes of energy exchange between different harmonics are resonant. These processes are comparable to one another in efficiency. As the result of this, the cascade-like multiplication of spectral components goes on during the wave propagation. In the space – time representation, the nonlinear broadening of the spectra corresponds to formation of discontinuities in the wave profile or weak shock waves with a front of finite width in a dissipative medium [1].

From the standpoint of nonlinear wave physics, the intense disturbance with a sawtooth-shaped profile is unique and therefore is the most interesting subject of investigation in nonlinear acoustics.

One can define the sawtooth wave as a travelling disturbance whose time profile contains both discontinuities and smooth sections. Any periodic disturbance propagating through a nondispersive medium transforms its shape to a sawtooth one at large distances. In doing so in quadratically nonlinear media the plane wave takes the form of a 'saw' with triangular 'teeth'. The dynamics of the transformation of the periodic signal into a 'saw' are shown in Fig. 1a. As the distance x increases, the fine details in the initial wave profile disappear smoothly during the wave propagation. The profile is the same for both a harmonic initial disturbance (curve *1*) and a more complicated signal (curve *2*) at some distance from the source of the order of several characteristic lengths ($x = x_2$ in Fig. 1).

A single time-limited disturbance transforms itself into an N-wave (Fig. 1b) at large distances in quadratic non-

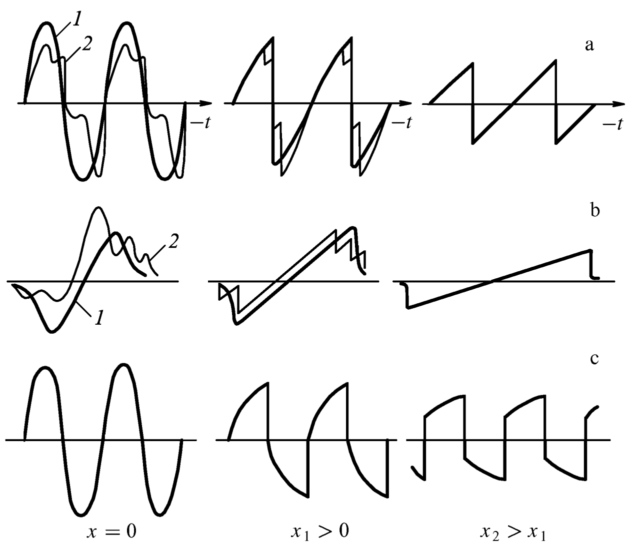

Figure 1. Formation of sawtooth-like waves: (*1*) harmonic initial disturbance; (*2*) complicated signal.

linear media. The integral of the function describing the wave profile tends to zero as $x \to \infty$ as a result of diffraction which is essential because real disturbances are limited in space.

In cubically-nonlinear media the 'teeth' of the 'saw' have a trapezoidal form (Fig. 1c). Each period contains two shocks: compression and rarefaction.

The existence of sawtooth-shaped waves other than those shown in Fig. 1 is possible in media with intricate nonlinear, dissipative and dispersive properties. However, the disturbances in Fig. 1 are most typical.

It is significant that the wave profiles mentioned above are asymptotically general for the wide range of initial disturbances. After its formation, the sawtooth wave remains quasistable. Only certain of the parameters may vary at later propagation. The peak pressure varies for periodic 'saws', with single pulse changes both in the peak pressure and the duration of the pulse. The wave profile is relatively stable and varies insignificantly with superposition and nonlinear interaction of the 'saws', as well as with the weak influence of complementary effects such as diffraction, dispersion, low-frequency modulation, etc.

Consequently, the sawtooth wave is a widespread wave type, whose stability is connected with the strong manifestation of nonlinear properties of the medium.

In nonlinear wave physics another object having nonlinear properties which are strongly expressed is more famous. That is the soliton, whose stability is provided by the competition between dispersion and nonlinearity. However, the soliton is stable only in ideal conservative systems, in the strict sense, whereas quasistability of 'saws' takes place in real dissipative media.

While on the subject of interactions between 'saws' or solitons, one can draw an analogy to the theories of hydrodynamic turbulence. It is known that in wave physics two kinds of nonlinear phenomena can be separated: those attributable to weakly expressed nonlinear effects (an example is phonon gas behaviour in solids with regard to lattice nonlinearity) or, on the other hand, those connected with the strong expression of nonlinear effects.

In a like manner there are two ways of looking at turbulence: as on the ensemble of weakly interacting quasiharmonic disturbances or, on the other hand, as on the set of interacting vortex structures, where each vortex is essentially a nonlinear object itself.

The second approach to turbulence is analogous to the approach to the problem of the interaction of wave objects with strongly expressed nonlinear properties such as sawtooth-shaped waves or solitons.

But, whereas the interactions between solitons are described in great detail in many reviews and monographs, sawtooth waves have received only a little consideration.

A number of principal experimental works devoted to sawtooth wave formation, as well as to nonlinear absorption and saturation effects, were completed at the end of the 1950s [2–6].

In recent years new phenomena were experimentally observed and explained: namely, self-focusing of sawtooth waves [7–13], self-refraction of pulses [14, 15], the existence of a physical limit for the peak acoustic pressure in the focal region [16] and some others. Furthermore, many of the known phenomena like parametric interaction, signal suppression and amplification, isolated wave collision, etc., happen quite differently for sawtooth waves than for quasiharmonic waves or solitons. These phenomena were studied in detail recently, because of their specificity. To describe the sawtooth wave, special mathematical approaches were developed, which are distinct from the common approaches used in other divisions of nonlinear wave theory.

The interest in these phenomena is associated with the numerous applications. Among the 'hot' problems one can emphasise the nonlinear methods of nondestructive testing and diagnostics in industry [17]; medical problems (disintegration of kidney stones and other mineral objects of biological origin [18, 19]); sonic boom and high-power acoustic noise [20, 21] (the ecological impact of these waves is under study now in connection with the design of a new generation of supersonic passenger aircraft [22, 23]). The references to the works which illustrate the connection between the discussed phenomena and the topical applied problems will be given where appropriate in later sections of this review.

2. Field and spectral approaches in nonlinear wave theory

2.1 General remarks

It is known that nonlinear waves in weakly and strongly dispersive media require different approaches for their description. When the medium has weakly expressed dispersive properties or dispersion is absent altogether, that is, propagation velocities of different components of the wave spectrum are close to or coincide with each other, the collinear harmonics can interact resonantly and exchange energy effectively in the process. This leads to cascade-like multiplication of harmonics and to broadening of the spectra. In other words, any virtual disturbance whose production is allowed by the type of nonlinearity can actually be created during the process of interaction and has an impact on the energy exchange.

Two possibilities exist here. One can describe the wave field using a temporal–spatial representation or by use of complex amplitudes for each spectral component, keeping track of the space variation of these amplitudes. It is evident that if the wave contains a great number of harmonics or the wave spectrum is continuous, the second (spectral) approach is inconvenient. When the analytical calculations are carried out, this method is effective only for the strongly dispersive media (for strictly specified frequency dependences of phase velocity agreeing with the initial wave spectrum) in the case of a small number of interacting harmonics. Examples are provided by classic problems of nonlinear optics [24]. To arrange the effective generation of the second harmonic in a quadratic nonlinear medium, it is necessary to use a birefringent crystal with 'the direction of synchronism'. Two harmonics at frequencies ω and 2ω which are differently polarised as ordinary and extraordinary waves, and are travelling in that direction, have approximately equal phase velocity and can effectively exchange energy. At the same time the virtual higher harmonics 3ω, 4ω, ..., the creation of which is permissible as a result of the series of cascade-like processes in the quadratic nonlinear medium, have strongly different phase velocities. These harmonics cannot grow in amplitude up to the values which allow their participation in the redistribution of energy throughout the spectrum.

A correct line of the spectral approach to the problem of wave interaction in dispersive media reduces to the following procedure. Originally, the problem was posed, for example, to arrange the resonant triplet $\omega_3 = \omega_1 + \omega_2$ to transform the energy from the pump wave ω_3 to the lower frequencies ω_1 and ω_2. Thereafter, the conditions must be found for the continuation of this resonant process, and in particular, a medium with the proper dispersive characteristic. Finally, the simplified evolution equations for the complex amplitudes A_1, A_2, A_3 of the resonant triplet must be derived in accordance with the real problem that was set.

Of course, the inverse sequence of operations is possible. Let a nonlinear medium with known dispersive properties be available. Analysing the form of the dispersive characteristics, one can decide easily which of the virtual interactions will be resonant and whether they exist in this medium in principle. Thereafter, the spectrum of the initial signal must be determined and corresponding equations derived for the amplitudes of the waves taking part in resonant interactions.

However, in many papers authors limit the wave spectrum or the number of interacting harmonics, without regard for the dispersive properties of the medium. In doing so, they impose on a nonlinear process artificial conditions different from the real ones. Nonlinear equations for spectral components derived in this case can be easily solved, because they are much more simple in comparison with the correct and more general equations governing the wave field. The results obtained in this manner may be interesting for mathematical theory, but physical results are often in rather poor agreement with the real observational data.

It is important to recognise the possibilities of both spectral and field approaches to solving the problems of wave interaction for those situations where both approaches can be used interchangeably: for acoustic waves, surface disturbances on shallow water, waves in plasma, in particle streams, etc. In addition, a demand arose recently in nonlinear optics to use the field approach for the description of broadband signals, namely, femtosecond laser pulses [25]. It seems likely, on the other hand, that acoustic analogies of nonlinear processes in optics call for investigation by the spectral approach [26].

Clearly, an active exchange of ideas and methods between different divisions of nonlinear wave physics must be accompanied by the taking account of the peculiar features of the considered phenomena.

In Sections 2.2 – 2.4 examples of nonlinear processes are given, described within the framework of the field and spectral approaches. It is interesting to compare results obtained by means of these two methods and to establish their correspondence to experimental data.

2.2 Harmonics generation

The propagation of a plane wave in a nonlinear medium without dispersion and dissipation can be described by the Riemann wave equation [1]:

$$\frac{\partial u}{\partial x} - \frac{\varepsilon}{c_0^2}\, u \frac{\partial u}{\partial \tau} = 0 \,. \tag{1}$$

Here u is the particle velocity, c_0 is the equilibrium velocity of sound, ε is a parameter of nonlinearity, x is the distance traversed by the wave, $\tau = t - x/c_0$. The field equation (1) describes realistically the observed phenomena, namely, a leading front steepening up to a discontinuity formation, generation of harmonics and combination frequencies, etc. In particular, if the harmonic signal $u = u_0 \sin \omega t$ is given at the input $x = 0$, from Eqn (1) the Bessel – Fubini solution for amplitudes of harmonics $n\omega$ $(n = 1, 2, 3, \ldots)$ follows:

$$B_n(x) = \frac{u_0 2 J_n(z)}{z}\,, \qquad z = \frac{\varepsilon \omega u_0 x}{c_0^2}\,, \tag{2}$$

which is in close agreement with the measured results. In solution (2) $J_n(z)$ are normal (at $z \leqslant 1$) or incomplete (at $z > 1$) Bessel functions [27].

If the spectrum is restricted artificially by two first harmonics and one seeks the solution of Eqn (1) in the form

$$u = B_1(x) \sin \omega\tau + B_2(x) \sin 2\omega\tau \,,$$

a pair of reduced equations can be obtained:

$$\frac{\mathrm{d}B_1}{\mathrm{d}x} = -\frac{\varepsilon\omega}{2c_0^2} B_1 B_2 \,, \qquad \frac{\mathrm{d}B_2}{\mathrm{d}x} = \frac{\varepsilon\omega}{2c_0^2} B_1^2 \,. \tag{3}$$

The solution of Eqns (3),

$$B_1 = \frac{u_0}{\cosh(z/2)}\,, \qquad B_2 = u_0 \tanh\frac{z}{2}\,, \qquad z = \frac{\varepsilon}{c_0^2}\, \omega u_0 x \tag{4}$$

provides the correct result (2) at small distances $z \ll 1$ only. But at $z \ll 1$ there is no sense in using reduced Eqns (3), because the result can be obtained with the same accuracy just from Eqn (1) by the successive approximation method, when the first harmonic amplitude is taken as the constant: $B_1 = u_0$. Over the region $z \geqslant 1$ where the reduced Eqns (3) could give the new information in principle, they describe the wave interactions inexactly. The behaviour of the first two harmonics is incorrect and higher harmonic generation is ignored completely (see Fig. 2).

2.3 Degenerate parametric interaction

Let us consider an interesting and beneficial example to demonstrate the special features of nonlinear phenomena in the sawtooth wave fields. The degenerate parametric interaction is a process which has been much studied for the waves in dispersive media.

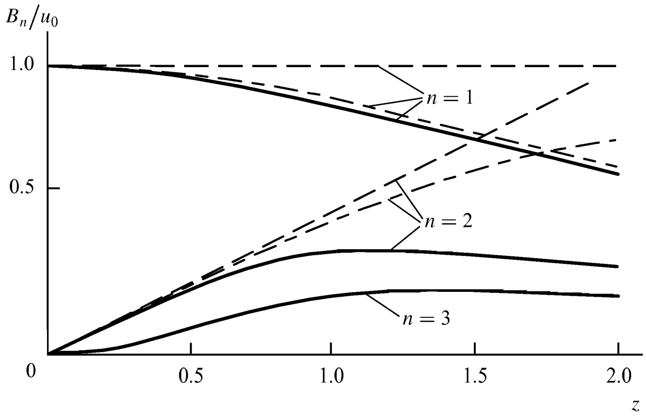

Figure 2. Amplitude of the harmonics calculated by the successive approximation method (dashed curves) and on the basis of reduced Eqns (3) (long-short dashed curves). Solid curves correspond to the exact solution (2).

It is known that quasiharmonic signals with frequency and wave vectors interrelated by the law of dispersion are stable wave objects in strongly dispersive media. For some specifically selected forms of dispersive characteristics one can create conditions for effective energy exchange between only two waves: the fundamental frequency ω_0 and subharmonic $\omega_0/2$. Such conditions can be achieved, for example, in nonlinear optical crystals for laser beams. Resonant interaction between the intense pump wave ω_0 and a weak signal $\omega_0/2$ (Fig. 3a) is a phase-sensitive effect. At optimum phase shift one can reach almost full concentration of energy in the signal wave and achieve by this means a large coefficient of parametric amplification, $K \gg 1$ [1].

At first glance it would seem that in the solution of the problem of interaction between waves ω_0 and $\omega_0/2$ one should take account of pump energy losses through the generation of its own higher harmonics. In fact, the 'parasitic'

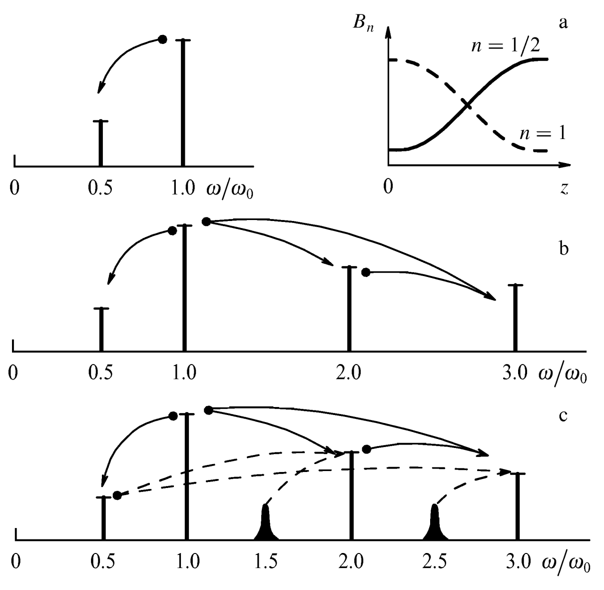

Figure 3. Basic directions of energy flow at the interaction of pump wave and subharmonic signal (a), taking into consideration the higher harmonics of the pump wave (b) and higher subharmonics (c).

channel of energy rejection, $\omega_0 \to 2\omega_0 \to 3\omega_0 \ldots$, may depress the beneficial process, $\omega_0 \to \omega_0/2$ (Fig. 3b), significantly. According to calculation [28], the amplification factor K cannot be greater than $K = \Gamma^{-1/2}$. Here $\Gamma = b\omega_0/(2\varepsilon c_0\rho_0 u_0)$ is the inverse acoustic Reynolds number (Goldberg number) which is equal to the ratio of characteristic shock formation path length $x_s = c_0^2/(\varepsilon\omega_0 u_0)$ to the absorption length $x_a = 2c_0^3\rho_0/(b\omega_0^2)$, where b is an effective parameter of the dissipation. It follows that, for example, at numbers $\Gamma \sim 10^{-2}$ which can easily be reached in laboratory experiments, amplification may be significant: $K \sim 10$.

However, this conclusion is incorrect. It was surprising because an infinite number of interacting waves was taken into account in the calculation [28], namely, all the multiple harmonics $n\omega_0$ ($n = 1, 2, 3 \ldots$) as well as the subharmonic signal $\omega_0/2$. It turned out that it was necessary to take into consideration all the higher subharmonic components $3\omega_0/2$, $5\omega_0/2$, ..., to obtain the correct result. Each of these subharmonics has very small amplitude, compared to the pump harmonics $n\omega_0$, and the losses due to their generation are insignificant. However, higher subharmonics open new channels for the transmission of energy from the basic subharmonic (i.e. from the signal to be amplified) up through the spectrum.

As a result of these processes, shown in Fig. 3c by dashed lines, the amplification is not practicable and the factor $K = 4/\pi \approx 1.28$ [29] barely exceeds unity. The result is known for nonlinear waves in long electric circuits [30].

The pattern of interaction of the great number of harmonics and subharmonics is too cumbersome because the spectral approach is inconvenient for the description of nonlinear waves in media without dispersion. If one follows the distortion of the time-profile during wave propagation, it turns out that the pattern is very simple. In Fig. 4 curve *1* illustrates the initial profile:

$$\frac{u}{u_0} = \sin\omega_0 t + 0.2\sin\left(\frac{\omega_0 t}{2} + \frac{\pi}{2}\right), \tag{5}$$

which is the sum of the pump and the half-frequency signal. The phase shift $\pi/2$ is given, such that amplification is optimal. Curves *1–11* in Fig. 4 correspond to growing distances $z = x/x_s$: 0, 0.5, 1, 1.5, 2, 3, 4, 6, 10, 15, 30. During wave propagation the accumulating nonlinear distortion leads to shock front formation. Because initial disturbance (5) has two nonsymmetric half-periods, this leads to asymmetry of the fronts relative to the zero level. Two neighbouring fronts move relative to each other, collide as absolutely inelastic particles and stick together [1]. In consequence of the collision of the fronts, the period of the resulting wave (curve *11* in Fig. 4) is doubled in comparison with the pump wave period. So, one can observe the parametric division of the frequency into two.

If required, these distorted profiles can be expanded into Fourier series and the whole spectrum of the wave field can be obtained (Fig. 5). It is clear that all the higher harmonics are comparable in amplitude, but the basic signal $\omega_0/2$ can be amplified insignificantly above its initial value, and amplification takes place only in a limited region of distances.

It is not to be supposed from the above that one cannot reach a marked amplification in nondispersive media at all. Evidently, higher subharmonic generation is possible only with the presence of the input signal $\omega_0/2$. There is a great

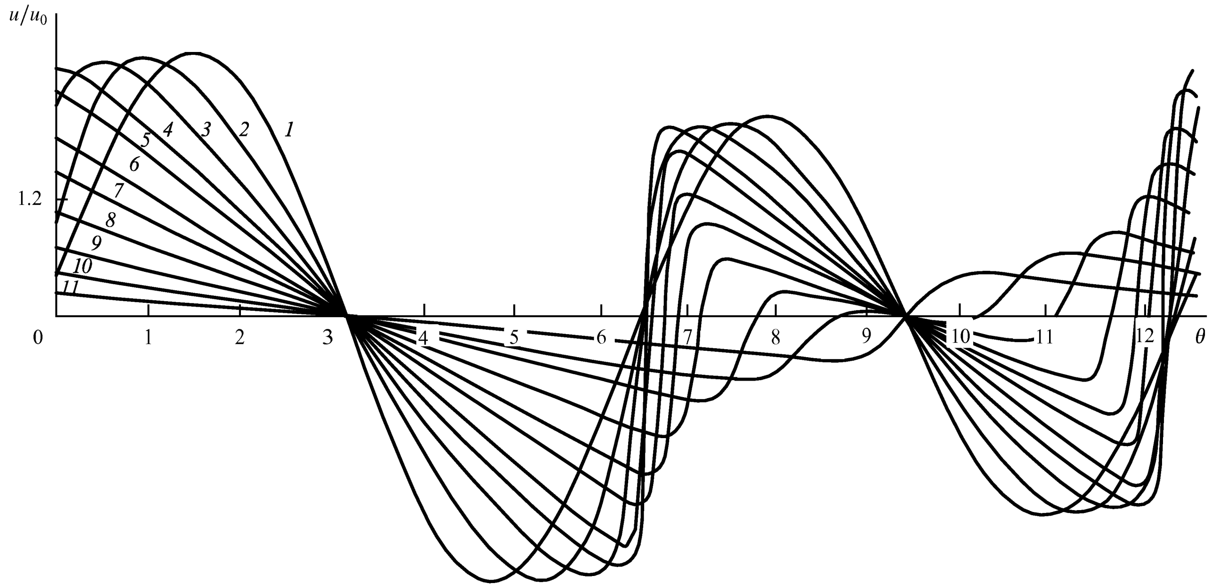

Figure 4. Wave profile for degenerate parametric interaction.

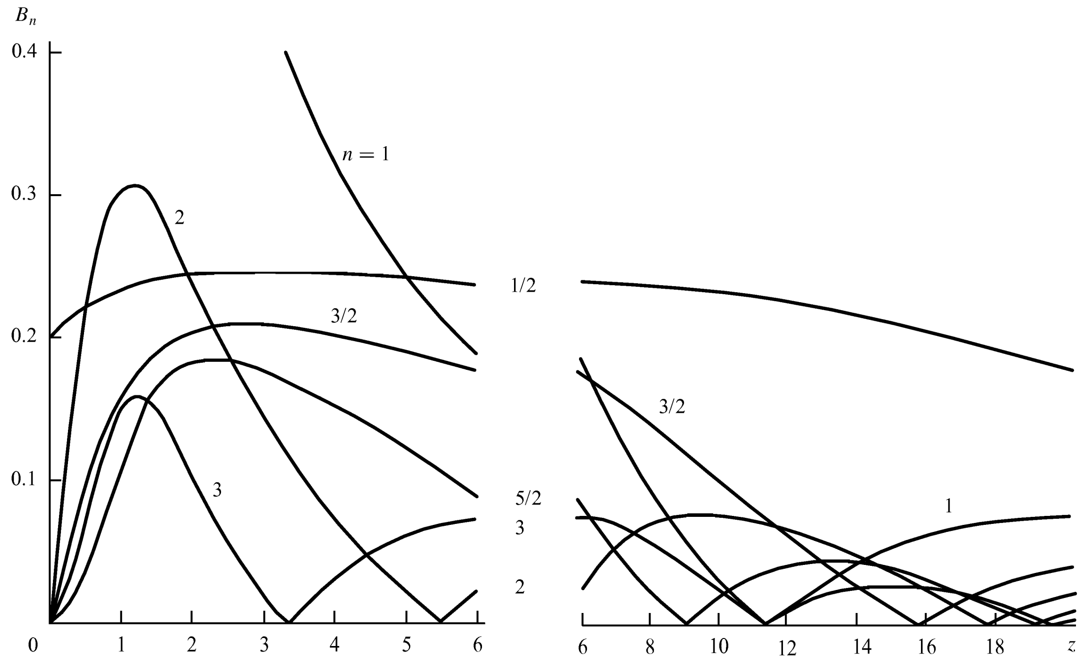

Figure 5. Wave spectrum for degenerate parametric interaction.

number of such subharmonics. Because of this, it is possible to extract information about the signal from all the spectral components by summing their contributions. Using special methods of signal processing, one can achieve a considerable effect [32].

In Fig. 6 a possible experimental scheme is shown [31]. The pump wave ω_0 propagates in insulated reference channel *2*, as well as in open receiving channel *1* where it interacts with the signal wave $\omega_0/2$. At the input of channel *2* the profile takes the form of symmetric 'saw' whose spectrum contains only integer frequencies $n\omega_0$. At the input of channel 1 the 'saw' has asymmetric fronts arranged in pairs; its spectrum contains both harmonic and subharmonic components. Subtracting two 'saws' at the inputs 1 and 2, we have the difference signal in the form of two peaks for each period, opposite in sign. The maximum pressure in these peaks is comparable with amplitude of the pump wave, that is, strong amplification is obtainable.

It was demonstrated with this example that the interaction pattern in dispersionless media is very specific and inaccessible. It is difficult to understand it without resorting to the analysis of the wave profile transformation, if attention is restricted from the outset to consideration of the spectra.

2.4 Inertialess self-focusing in cubically nonlinear nondispersive media

This is an example of why the spectral approach prevents the production of correct results for the sawtooth wave beams.

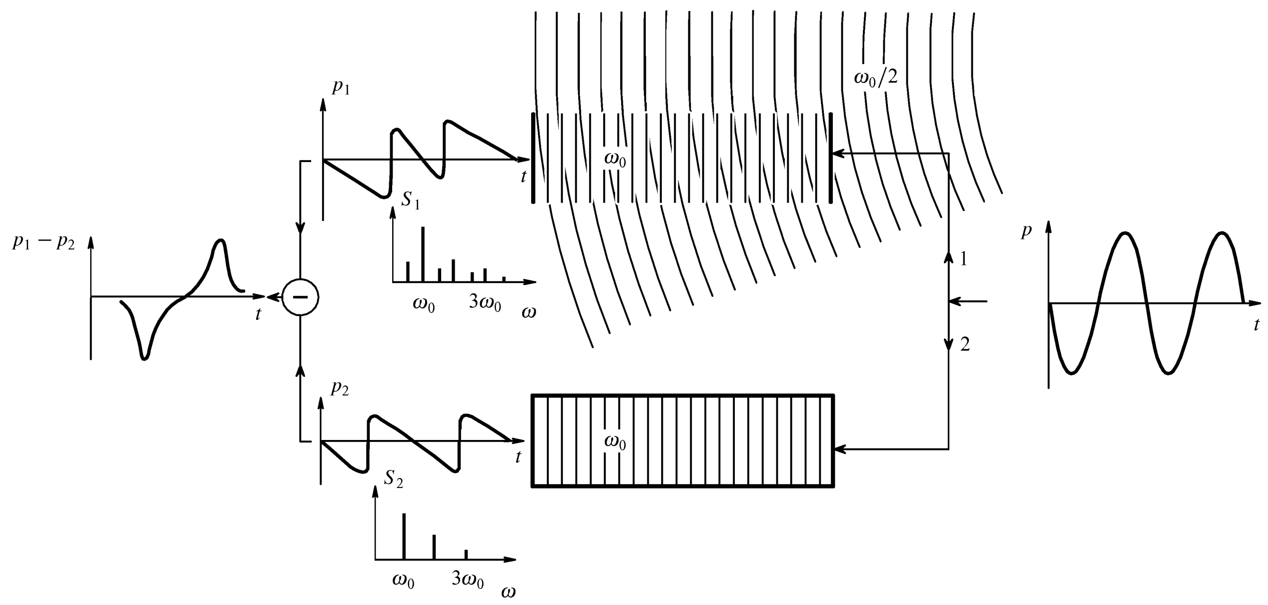

Figure 6. Experimental scheme which allows significant amplification of the signal in media without dispersion.

Space-limited beams exposed to diffraction and self-action effects can be described by the equation [11, 12]

$$\frac{\partial}{\partial \tau}\left[\frac{\partial u}{\partial x}+\gamma u^2\,\frac{\partial u}{\partial \tau}-\frac{b}{2c_0^3\rho_0}\,\frac{\partial^2 u}{\partial \tau^2}\right]=\frac{c_0}{2}\Delta_\perp u\ . \qquad (6)$$

Here γ is the coefficient of cubic nonlinearity, and the Laplacian $\Delta_\perp$ is taken with respect to the transverse coordinates. To describe the shock front correctly, the dissipative term in Eqn (6) is held proportional to b. However, it is assumed that fronts are infinitesimally thin and $b \to 0$; there is a singular perturbation problem containing the small parameter for the highest order derivative [31].

Following the spectral approach formally one can seek a solution of Eqn (6) as a harmonic wave,

$$u = A(x, \boldsymbol{r}_\perp)\,\exp(\mathrm{i}\omega\tau) + \text{c.c.} \qquad (7)$$

For complex amplitude A the nonlinear equation of Schrödinger type can be obtained [33, 34]:

$$\mathrm{i}\omega\,\frac{\partial A}{\partial x}=\frac{c_0}{2}\,\Delta_\perp A+\gamma\omega^2|A|^2 A\ . \qquad (8)$$

It is known that Eqn (8) describes the instability of the initial plane wavefront in cases where its intensity exceeds a critical value [34]. Then the amplitude of any spatial perturbation harmonic (perturbation being an addition to the plane nonlinear wave amplitude) grows exponentially as a function of distance x. Thus, in a self-focusing medium ($\gamma > 0$) the plane wave is unstable; it breaks down into separate focusing beams each carrying a power of the order of the critical one [34].

On the other hand, one can seek a solution of Eqn (6) as a plane wave:

$$p = p(x, \tau)\ . \qquad (9)$$

The solution of Eqn (6) [35] corresponding to formula (9) describes the transformation of the initial harmonic wave into a sawtooth one (see Fig. 1c), each 'saw' of which has a trapezoidal form. As a result of nonlinear absorption within the thickness of the shock fronts the peak values of the wave (amplitudes of the 'saws') decay with distance according to the law [13, 35]

$$A(x) = A_0(1 + c\gamma\omega A_0^2 x)^{-1/2}\,, \qquad c = \frac{3 - 2\ln 2}{4\pi}\ . \qquad (10)$$

In this way, two opposite processes (increase in amplitude because of self-focusing and nonlinear absorption owing to shock front formation) are being described by one, and only one nonlinear term in Eqn (6). Evidently, the transition from (6) to (8) on the basis of assumption (7) is incorrect; here adequate methods for analysis are required, which take into consideration the special features in the behaviour of the sawtooth-shaped waves.

Corresponding approaches and results are described in Ref. [13]. In particular, at the stage where the developed trapezoidal 'saw' does exist one can obtain, using the nonlinear geometric acoustics approximation, the following system for the intensity $J = \overline{u^2}$ averaged over the period:

$$\frac{\partial J}{\partial x}+\frac{\partial}{\partial r}\,(JV)+\frac{1}{r}\,JV=-\alpha\omega\gamma J^2\ , \qquad (11)$$

$$\frac{\partial V}{\partial x}+V\,\frac{\partial V}{\partial r}=\gamma c_0\,\frac{\partial J}{\partial r}\ . \qquad (12)$$

The second variable $V = \partial\psi/\partial r$ (where ψ is an eikonal) is the angle of inclination of the ray to the beam axis; α is the constant determined by the structure of the profile of the saw-tooth wave. It is interesting to note that the nonlinear term ($\sim \gamma$) in Eqn (6) caused the appearance of the right sides in Eqns (11) and (12) simultaneously. The right side in Eqn (12) is responsible for the nonlinear bending of rays and the self-focusing effect, but the right side of Eqn (11) is responsible for nonlinear absorption. The system (11), (12) is analogous to the equations describing one-dimensional flow of compressible liquid in the form used for the description of aberration self-focusing of light [33]. However, in the optical problem the absorption can be absent and right side of Eqn (11) is equal to zero. But in the case being considered at $\gamma \to 0$ not only will the nonlinear absorption disappear, but self-focusing as well.

As the analysis [13] of both Eqn (6) and the system (11), (12) has shown, the self-focusing process develops over lengths well in excess of the shock formation scale. Here the wave profile has a trapezoidal sawtooth shape. There is competition between two processes, self-focusing and damping, both generated by the same nonlinearity. As a result, the width of the beam may be reduced substantially while the amplitude of the 'saw' increases little.

In summary it may be said that there exist principal distinctions between beam self-action processes in dispersive and nondispersive media. This calls for different approaches and description techniques.

3. Diffracting beams of sawtooth-shaped waves

The wave interactions were studied up to the beginning of the 1970s on the basis of simple theoretical models. One-dimensional waves were considered mainly — plane, spherical, and cylindrical. But in real situations one has to deal with beams, and diffraction effects must be taken into account.

The peculiarities of the behaviour of nonlinear space-limited beams were noted early in the experiments [2–5]. Systematic studies, however, were begun later [36, 37], after adequate theory was developed to check it.

In Fig. 7 the profile of an initially harmonic signal is shown measured [37] at different distances from the ultrasonic source in water. A piezoceramic disk, 30 mm in diameter, has been used as a radiator of 1 MHz resonant frequency. The signal was received by a broadband hydrophone (piezoquartz plate, x-cut) of 10 mm diameter and 14.5 MHz resonant frequency. One can see that at small distances the signal is similar to the harmonic one. Furthermore, the front becomes more steep and there appears an asymmetry in the distortion of both compression and rarefaction half-periods. At a distance of 25 cm approximately, the shock is formed in the wave profile. This leads to the appearance of oscillations behind the front which are connected with resonant excitation of the hydrophone. In the further propagation one can observe nonlinear absorption of the wave, but its asymmetry is well-marked as before: the negative half-period is smoothed and expanded, but the positive one is shortened and sharped.

In a series of experiments (see, for example, Ref. [38]) 'smoothing' of the transverse distribution of the acoustic field in a beam has been observed. Near the axis the shock wave forms earlier, and the intense absorption takes effect in the paraxial region. At the same time, the shocks do not yet exist in regions distant from the axis and wave amplitude is constant. So, the stronger absorption near the axis leads to broadening of the beam, and the wave transforms into a plane wave of small amplitude — the radial distribution becomes more homogeneous [39]. This phenomenon is analogous to the process of nonlinear 'smoothing' of the directivity pattern of a high-power acoustic radiator, which was considered in Ref. [40].

The processes of nonsymmetric distortion of diffracting nonlinear waves were studied in detail in numerical experiments [41] where the excess of positive peak pressure over its initial value has also been observed.

The theoretical investigations of nonlinear effects taking diffraction into consideration were begun after Khokhlov suggested supplementing the slowly varying profile method [42] with the quasi-optic approximation, the ideas of which

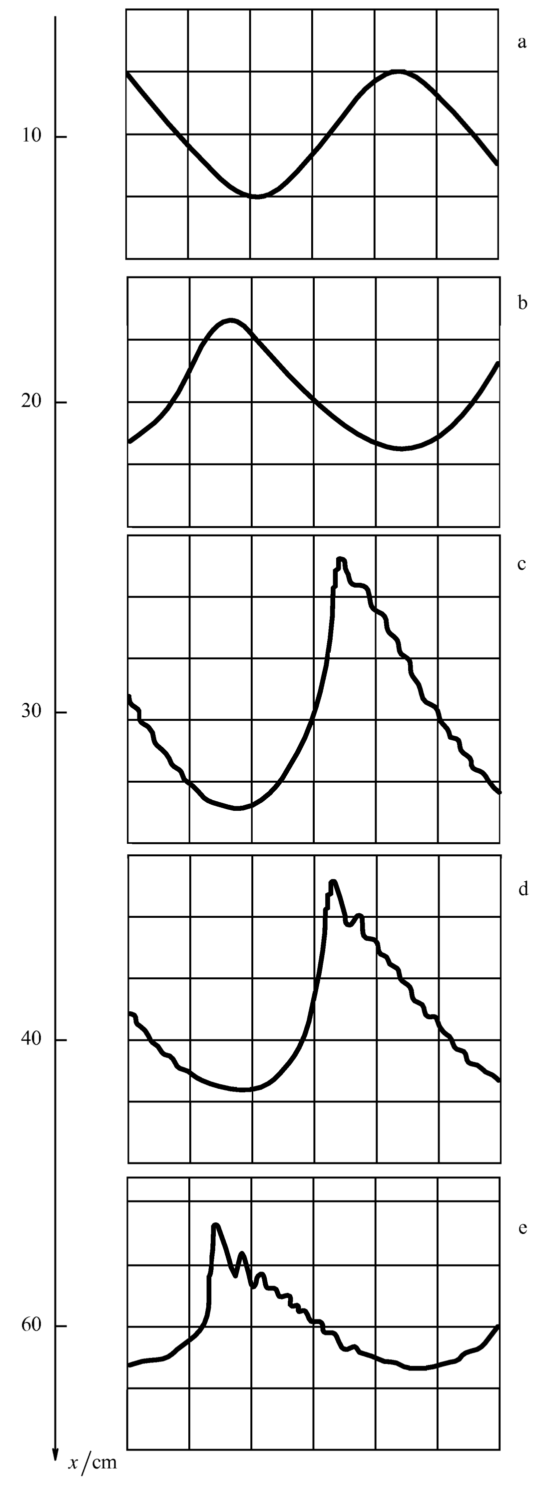

Figure 7. Nonlinear distortion of the wave form on the axis of a beam with increase in distance x from the source. $I = 0.9$ W cm^{-2}; $N = 2.5$; graduation on horizontal scale 0.2 μs, on vertical: (a, b) 2.8 atm, (c–e) 1.1 atm.

originate from the works by Leontovich and Fok on radiowave propagation along the Earth's surface. After the simplification, the system of equations of mechanics of compressible media was reduced to the single equation [43]

$$\frac{\partial}{\partial \tau}\left(\frac{\partial p}{\partial x} - \frac{\varepsilon}{c_0^3 \rho_0}\, p\, \frac{\partial p}{\partial \tau}\right) = \frac{c_0}{2}\, \Delta_\perp p\,, \tag{13}$$

which we proposed to name the Khokhlov–Zabolotskaya equation (KZ). At the present time this name has come into common use. In Eqn (13) p is acoustic pressure, and other notations are the same as in Eqns (1) and (6).

The modified forms of this equation were suggested later.

In Ref. [44] the dissipative term which is posed inside brackets in formula (13) is taken into consideration (containing the second derivative of the field) — just the same as in Eqn (6). In Ref. [45] the dispersive term with the third derivative is taken into account, giving the opportunity to describe the space-limited solitons. In Ref. [46] the integral term is added, the kernel of which can be reconstructed for any frequency-dependent absorption and dispersion [47, 48].

More than 100 works are known to date which are devoted to calculation on the basis of the KZ equation or its modified forms. These are mainly numerical results [41] or data on harmonics and combination frequencies for weakly expressed nonlinearity [49–51]. The last works are of great applied importance for the calculation of parametric underwater devices [49, 52].

However, the present review is devoted to sawtooth waves, in beams of which nonlinear effects are expressed strongly. There are only a few works on this problem because of mathematical difficulties in their analytical and numerical treatment.

In Ref. [53] the approximate method was used for KZ Eqn (13) analysis, based on the power-series expansion of the solution in the small parameter, which is a ratio between the current value of radial coordinate r and the initial width a of the beam:

$$p(x, r, \tau) = p_0(x, \tau) + \frac{r^2}{2a^2} p_2(x,\tau) + \frac{r^4}{4a^4} p_4(x, \tau) + \ldots \,. \tag{14}$$

Such an approach is similar to the aberration-free approach used in the theory of laser self-focusing [53]. As distinct from the optical case, here the system of ordinary differential equations cannot be obtained, but the infinite chain of coupled partial nonlinear equations can. Restricting consideration to the first two equations of this chain ($p_4 = p_6 = \ldots = 0$), one can obtain the canonical system

$$\left(\frac{\partial}{\partial x} - \frac{\varepsilon}{c_0^3 \rho_0} p \frac{\partial}{\partial \tau}\right)\begin{pmatrix} p \\ F \end{pmatrix} = \begin{pmatrix} F \\ g(x) \end{pmatrix}, \qquad F = \frac{N}{2}\int p_2 \, \mathrm{d}(\omega\tau) \tag{15}$$

(here $p \equiv p_0(x,\tau)$ is the field on the axis) containing the nonlinear operator with the same principal part [54], which can be solved exactly. The function $g(x)$ in formula (15) is determined from the conservation of linear momentum of the wave, N is the number (the only similarity criterion in the KZ equation) equal to the ratio of shock formation length to the diffraction length [39]:

$$N = \frac{x_s}{x_d} = \frac{c_0^3/(\varepsilon\omega p_0)}{\omega a^2/(2c_0)} \,. \tag{16}$$

In dimensionless notation,

$$V = \frac{p}{p_0}\,, \qquad z = \frac{x}{x_s}\,, \qquad \theta = \omega\tau\,, \qquad R = \frac{r}{a}\,, \tag{17}$$

the KZ equation takes the form

$$\frac{\partial}{\partial\theta}\left(\frac{\partial V}{\partial z} - V\frac{\partial V}{\partial\theta}\right) = \frac{N}{4}\left(\frac{\partial^2 V}{\partial R^2} + \frac{1}{R}\frac{\partial V}{\partial R}\right) . \tag{18}$$

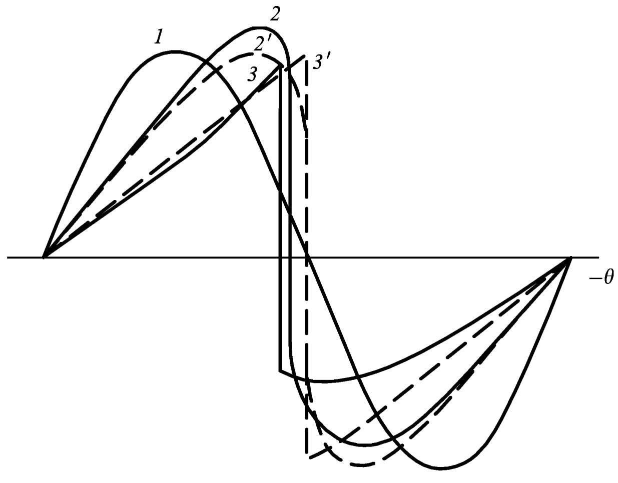

Figure 8. Influence of diffraction phase shift on the change in behaviour of the wave in the beam (solid curves) in comparison with the plane wave (dashed curves) at $N = 0.4$.

In Fig. 8 results are presented of graphical analysis of the solution of the system (15) on the beam axis at number $N = 0.4$. The curve *1* shows the wave profile at $z = 0$. In the case that the wave is plane, the nonlinear effects lead to the profile distortion shown by curves *2*$'$ ($z = 1$) and *3*$'$ ($z = 2$). In the presence of diffraction the wave behaviour is different: the positive half-period decreases in duration, but the negative increases. Since the areas must be equal for both half-periods, the excess of positive pressure over the initial value (curve *2*, $z = 1$) takes place in some region of distance x near x_s. The excess pointed out will be 'cut off' in the shock existence region $x > x_s$ by the moving front, but the distinction from the plane wave (curves *3* and *3*$'$) manifests itself more significantly.

These phenomena are not connected with the self-action [33] or with the more intense generation of harmonics in the beam [55] than in the plane wave. These phenomena can be explained easily on the basis of the distinctions in diffractional phase shifts or propagation velocities between fundamental and higher harmonics [48]. In the case of open resonators, for example, the analogous shifts will cause the splitting of frequencies of different transverse modes [48].

However, the direct expansion of the sound field in series (14) in the transverse coordinate with only two terms (15) taken into account sets a strong restriction on the feasibility of the results obtained. It turns out that the solutions describe the processes precisely near the axis, but at small distances only, in comparison with the length of diffraction.

To eliminate this difficulty, in Ref. [56] the method [53] was modified in the following way. The solution of Eqn (18) was sought in the form

$$V = V\big[z, R, T = \theta - \psi(z, R)\big] \,, \tag{19}$$

where ψ is an unknown function describing the curvature of the wave front. In place of the KZ equation, the following system has been obtained:

$$\frac{\partial}{\partial T}\left[\frac{\partial V}{\partial z} - V\frac{\partial V}{\partial T} + \frac{N}{4}\left(V\Delta_\perp\psi + 2\frac{\partial V}{\partial R}\frac{\partial\psi}{\partial R}\right) - \frac{N}{4}\frac{\partial V}{\partial T}Q\right] = \frac{N}{4}\Delta_\perp V \,, \tag{20}$$

$$\frac{\partial\psi}{\partial z} + \frac{N}{4}\left(\frac{\partial\psi}{\partial R}\right)^2 = \frac{N}{4}Q(z,R) \,. \tag{21}$$

Here Q is an arbitrary function. Choosing Q from considerations of simplicity (as in the linear quasi-optic diffraction theory, for example) and using the paraxial expansion (14) for both functions V and ψ, one can obtain the solution on the beam axis in the parametric form $V = V(T_0)$, $T = T(T_0)$:

$$V = \frac{1}{f}\sin(T_0 + \eta) + \frac{1}{2Nf}\int_0^\eta f(y)\sin(\eta - y)\,dy\ , \tag{22}$$

$$T = T_0 - \frac{1}{N}\int_0^\eta f(y)\sin(T_0 + y)\,dy$$

$$- \frac{1}{2N^2}\int_0^\eta f(y)\,dy\int_0^y f(y')\sin(y - y')\,dy'\ .$$

Here T_0 is the parameter, $f = (\cos\eta)^{-1}$, $\eta = \arctan Nz$.

The sawtooth wave formation process calculated from formula (22) is similar to the process shown in Fig. 8. The comparison shows [56] that the wave form (22) as well as the spatial harmonics distribution correspond closely to the numerical results at any distance from the source.

However, in the case where it is necessary to know the beam structure outside the paraxial region, the approaches of Refs [53, 56] are inapplicable. A simple asymptotic theory [57] was developed taking into account the influence of diffraction and nonlinearity on the Gaussian beams. Here the transition was used to the implicit 'Riemann variable' $T = \theta + zV$ which contains the unknown function V. Thereafter the nonlinear equations obtained were solved by the perturbation method for the diffracting beams. It turned out that both limiting cases (linear beams or nonlinear waves without diffraction) can be described exactly by this method even in the first approximation. In the intermediate region (for numbers $N \sim 1$) errors can appear at the distances where the shock formation process is accompanied by the transformation of the plane wave into a spherically diverging one.

In subsequent works the method [57] was refined with consideration for higher approximations [58]. A theory for non-Gaussian transverse profiles [59] was developed similar to the uniform or polynomial one. As distinct from Ref. [57], the perturbation method was used here along with the renormalisation procedure not only with respect to the time variable, but also to the transverse coordinates. A high accuracy was reached in Ref. [60] where the renormalisation procedure, which makes it possible to describe the sawtooth waves, was performed on the basis of three first approximations to quasilinear perturbation theory.

In conclusion to this section, Refs [60, 61] can be noted, where the region of applicability was analysed for the approach based on the KZ equation. This approach was shown to be correct for the description of results obtained during laboratory experiments. Recall that for nonlinear effects which are weakly expressed and where there are no shocks in the wave profile, the accuracy of the KZ equation is confirmed by underwater experiments as well as by calculation of real parametric devices [52].

Several tens of published works are devoted each year to the KZ equation and to diverse modifications of such field equations. Therefore, it is interesting to note that along with the line of investigation described above, which has its origin in classical works on wave theory, there exists probably a second independent line. It originates from the works by Prandtl on hydrodynamics (see, for example, Ref. [63]). In fact, the ideas used in the derivation of the boundary-layer equations (1904) are identical with the ideas of quasi-optical approximation. Their development provided the foundation in mechanics for the works, closely connected, in fact, with the works on nonlinear wave theory, but having essentially no influence on it. So, as early as 1948, the equation was derived [64] coincident with the KZ equation in this form, but the problem definition and the physical sense of the variables are different in these two cases. Instead of the wave profile and the transverse beam form at the source, in the 'flow around' problem one must specify the body's shape and the normal component of the stream velocity, which equals zero at the surface. In Ref. [65] a similar approach was used to calculate the transonic flow around the wing. Some reflection on the results [64] is presented in a book [63, p. 655] where the stationary version of the KZ-type equation is used in the derivation of the Karman near-sonic similarity law.

However, the continuation of the 'mechanical line' of investigation brought into existence the 'pure wave' works in which the KZ equation was derived once again. There are works on weak shock wave theory devoted to their focusing [66] and instability under transverse spatial modulation [67] (see also [63, p. 493]). It would be well to have an acquaintance with all of these works, because many of them contain important mathematical results or physical conclusions which can be extended to other subjects of investigation.

4. Waves in inhomogeneous media and nonlinear geometric acoustics

The tendencies today in fundamental research and applications of the theory of sawtooth waves put in the forefront the problems devoted to intense wave propagation through inhomogeneous media. The propagation of sonic boom pulses generated by supersonic passenger aircraft [68, 69], explosive waves in the atmosphere and in the ocean [70], continuous acoustic radiation from powerful sound transducers, etc., can provide examples of such problems.

All the problems arising here can be divided conventionally into three groups. There are problems connected with information transmission (an example — explosive waves in an underwater sound channel), and with intense wave action and environment protection from it (sonic boom), as well as inverse problems on nonlinear nondestructive testing and diagnostics (reconstruction of the parameters of the source, scatterers and medium through which the signal propagates).

To describe the sawtooth wave it is necessary to determine correctly the position and form of the shock front, as well as differentials in parameters across the front. For this purpose the gas dynamic methods used are simplified with regard to the small acoustic Mach numbers [71 – 73]. However, there is a little sense in having data for the wave front only. The wave has to be considered as a signal of complex spectral composition carrying information about the source and the medium. For example, during propagation in the atmosphere, ocean or ground the wave interacts with inhomogeneities acting as scatterers, natural waveguides, lenses, filters and having marked frequency-selective properties. It is necessary therefore to follow the distortion of the wave spectrum. To follow that for the spatial – temporal characteristics of the disturbance, one has to describe the evolution of the smooth section in the wave profile in parallel with the shock front, as well as their interaction with each other. This complex problem can be solved effectively only on the basis of nonlinear acoustic approximation with the use of results obtained in the linear theory of wave propagation through inhomogeneous media [74 – 76] and the theory of nonlinear nondispersive waves [1, 71 – 73].

Approximations of nonlinear geometrical acoustics type were developed and applied to the waves in smoothly-inhomogeneous media (see, for example, Refs [77 – 79]). In Refs [80 – 82] evolution equations of KZ-type were derived for inhomogeneous media that make it possible to take into account the diffraction of beams. However, these problems remain difficult in spite of simplification, and therein lies the explanation why the concrete results obtained here are few in number.

It is appropriate now to indicate the two methods for the simplification of the initial equations, which made it possible to solve nonlinear problems. The first method is based on the nonlinear geometric acoustics approximation; it is applicable to beams with a large ray divergence. However, it is not valid in aberration areas, where the rays intersect each other. The second approach is applicable only to beams with a narrow angular spectrum, but in return it gives a field in the vicinity of focuses and caustics.

The evolution equation was derived in Ref. [21] by means of the second approach:

$$\frac{\partial}{\partial\tau}\left[\frac{\partial p}{\partial s}-\frac{p}{2}\frac{\partial}{\partial s}\ln(\rho c)-\frac{\varepsilon}{c^3\rho}\,p\,\frac{\partial p}{\partial\tau}\right] -\frac{1}{2c^2}\left[(\bar{\xi}\nabla_\perp)^2 c\right]_{\bar{\xi}=0}\frac{\partial^2 p}{\partial\tau^2}=\frac{\rho}{2}\nabla_\perp\left(\frac{c}{\rho}\nabla_\perp p\right). \quad (23)$$

To describe the acoustic pressure field p in the vicinity of an arbitrarily selected ray, the curvilinear coordinates are used here. The distance s is measured along the ray from some fixed point, and the coordinates $\bar{\xi}=(\xi,\eta)$ are assigned in a special way in the cross section: the basis of this system is turned relative to the Frenet trihedral through an angle defined by the curvilinear integral of the ray torsion [21]. Parameters of the medium, i.e. sound velocity c, density ρ, and nonlinearity ε in Eqn (23) depend on space coordinates. It should be mentioned that the approach [21] makes it possible to generalise Eqn (23) for dissipative, relaxing and other media with arbitrary frequency dependences of their linear properties (in the same manner as was done in Ref. [46] for homogeneous media).

One can obtain for a periodic wave with a strongly distorted profile, in the nonlinear geometric acoustics approximation, the following equations:

$$(\nabla\psi)^2=\frac{c_0^2}{c^2}=n^2\,, \quad (24)$$

$$\nabla\psi\nabla p+\frac{1}{2}\,\Delta\psi p-\frac{p}{2}\,\nabla\ln\rho\,\nabla\psi-\frac{\varepsilon n}{c^3\rho}\,p\,\frac{\partial p}{\partial\tau}=0\,, \quad (25)$$

where $p=p(\tau=t-\psi(\mathbf{r})/c_0,\,\mathbf{r})$. Interestingly, the eikonal equation (24) has here the same form as in a linear problem. The validity of this agreement is evident for periodic signals. In fact, if the diffraction is negligible for the fundamental frequency wave, it has to be valid for its higher harmonics. The situation is different for modulated signals, where nonlinear propagation gives rise to low-frequency spectral components, and for intense acoustic pulses that already contain low frequencies at the input of the nonlinear medium. Sometimes it is convenient to modify the eikonal equation by including nonlinear terms. Such is the case when allowing for the self-action effects in a cubic nonlinear dispersionless medium [13] and for the movement of a shock front in the accompanying coordinate system [14 – 16].

Let us consider, for example, the two-dimensional problem, taking the eikonal ψ and the parameter α 'numbering' rays on the straight line $x=0$, as independent

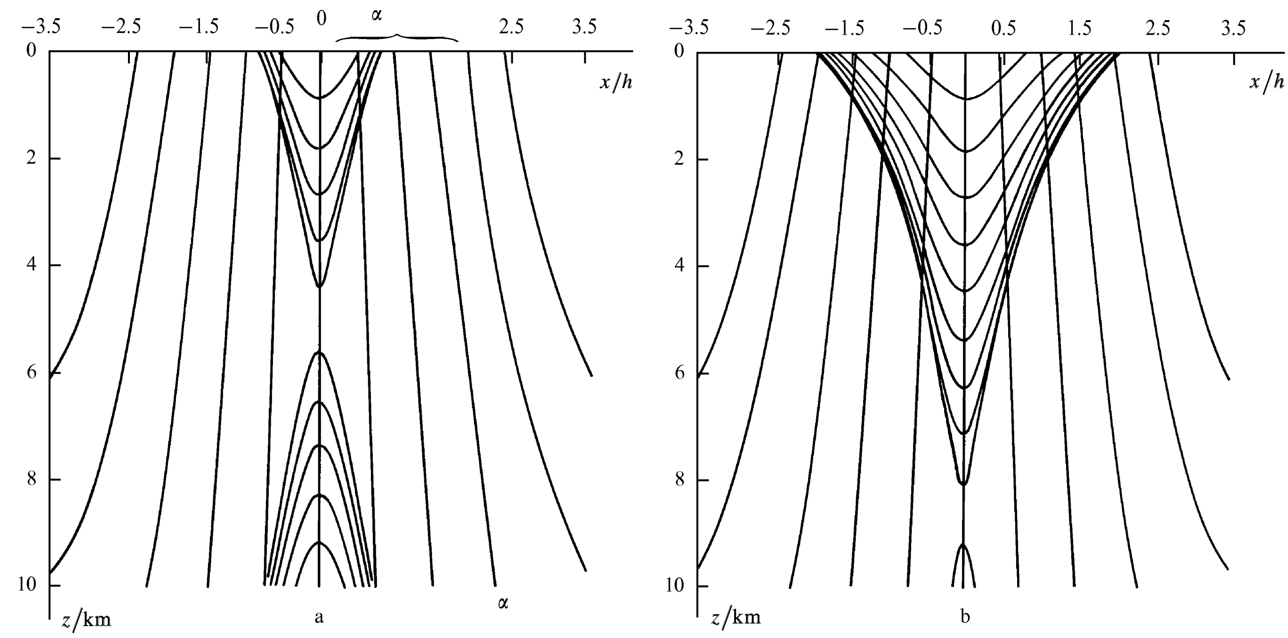

Figure 9. Rays and lines of equal levels of peak pressure for pulse signal (a) and periodic 'saw' (b).

variables (Fig. 9). In this case the system of Eqns (24), (25) can be reduced to the equation [83]

$$\frac{\partial p}{\partial \psi}+\frac{p}{2}\frac{\partial}{\partial \psi}\left[\frac{D(\alpha,\psi)}{\rho c^2}\right]-\frac{\varepsilon}{c_0 c^2 \rho}\,p\,\frac{\partial p}{\partial \tau}=0\,, \tag{26}$$

where $D=\partial(x,z)/\partial(\alpha,\psi)$ is a Jacobian of the transformation of the Cartesian coordinates x, z into the ray coordinates α, ψ. For a stratified medium in which parameters are dependent only on coordinate z, the solution of the eikonal Eqn (24) can be written in a convenient parametric form:

$$\psi(\alpha,z)=\psi_0(\alpha)+\int_0^z \frac{n^2(y)\,\mathrm{d}y}{[n^2(y)-a^2(\alpha)]^{1/2}}\,, \tag{27}$$

$$x(\alpha,z)=\alpha+a(\alpha)\int_0^z \frac{\mathrm{d}y}{[n^2(y)-a^2(\alpha)]^{1/2}}\,, \tag{28}$$

where the function

$$a(\alpha)=\left(\frac{\partial \psi}{\partial x}\right)_{z=0}=n_0\cos\theta_0=\frac{\partial \psi}{\partial x}=n\cos\theta=\mathrm{const}(\alpha) \tag{29}$$

describes the inclination of the α-numbered ray to the x-axis; θ is the angle between direction x and the tangent to the ray. One can fix the angle of departure for each ray after the function $a(\alpha)$ (29) is specified. The arbitrary wave front can be prescribed at the 'fan' of the constructed ray set. In this case the Jacobian is given by [83]

$$D=\frac{[n^2(z)-a^2(\alpha)]^{1/2}}{n^2(z)}\left\{1+\frac{\mathrm{d}a}{\mathrm{d}\alpha}\int_0^z \frac{n^2(y)\,\mathrm{d}y}{[n^2(y)-a^2(\alpha)]^{3/2}}\right\}. \tag{30}$$

We call attention now to the transport Eqns (25), (26). As distinct from the linear case they contain an additional time variable τ. This variable can be eliminated in linear problems by the transition from p to the complex amplitude A: $p=A(\mathbf{r})\exp(-\mathrm{i}\omega\tau)$. However, Eqns (25), (26) can describe an essentially nonharmonic wave with a wide spectrum of interacting Fourier components; it is impossible, in general, to eliminate τ for such a wave.

Nevertheless, in the most interesting case, when nonlinear effects are expressed strongly and the wave profile has the sawtooth-shaped form (see Fig. 1a), one can put

$$p(\tau,\mathbf{r})=-2f\tau A(\mathbf{r}) \tag{31}$$

and go from Eqns (25), (26) to the equations for the peak values A of the field p:

$$\nabla\psi\nabla A+\frac{A}{2}\,\Delta\psi-\frac{A}{2}\,\nabla\ln\rho\nabla\psi+\frac{2\varepsilon n f}{c^3\rho}\,A^2=0\,, \tag{32}$$

$$\frac{\partial A}{\partial \psi}+A\,\frac{\partial}{\partial \psi}\,\ln\sqrt{\frac{D}{\rho c^2}}+\frac{2\varepsilon f}{c_0 c^2 \rho}\,A^2=0\,. \tag{33}$$

Formula (31) describes the straight line section of the periodic 'saw' profile; f is fundamental frequency. Shock fronts are placed at $2f\tau_n=\pi(2n+1)$, $n=0,\ \pm1,\ \pm2,\ \ldots,$ and they cannot be displaced from the points τ_n during the wave propagation. Eqns (32), (33) can be linearised by the substitution $A=B^{-1}$ and can be easily solved.

For a bipolar N-pulse (see Fig. 1b) one can also use Eqns (32), (33). But in this case the variable A (31) has a sense of inclination of straight line sections of the wave profile, and both fronts will be shifted during the propagation to the positions $\tau=\pm T(\psi)$. To take into account these differences, we use the conservation of linear momentum [it follows from Eqn (26) evidently] and the connection between 'amplitudes' of N-wave (A_N) and 'saw' (A_s) [the last follows from Eqn (31)]:

$$\left(\frac{D}{\rho c^2}\right)^{1/2} A_N(\psi)T(\psi)=\mathrm{const}\,,\qquad A_N=2fTA_s\,. \tag{34}$$

Solving (33) for $A=A_s$ and using conditions (34), we obtain an analogous result for A_N.

For the planar layered medium whose properties depend only upon z, these solutions have the form [83]

$$A_{s,\,N}(\alpha,\,z)=\frac{A_0(\alpha)}{n}\left(\frac{D_0\rho}{D\rho_0}\right)^{1/2}$$
$$\times\left\{1+\frac{1}{l_s}\,\frac{A_0(\alpha)}{p_0}\int_0^z\left[\frac{D_0\rho_0\varepsilon^2}{D\rho\varepsilon_0^2}\,\frac{n^6}{n^2-a^2(\alpha)}\right]^{1/2}_{z=z_1}\mathrm{d}z_1\right\}^m\,. \tag{35}$$

In formula (35) $m=-1$ corresponds to a periodic 'saw', but $m=-1/2$ to an N-wave. The characteristic nonlinear length (or shock formation distance) is $l_s=c_0^3\rho_0/(2f\varepsilon_0 p_0)$; for the bipolar N-pulse it is convenient to put here $f=(2T_0)^{-1}$, where T_0 is the initial duration of compression (or rarefaction) phase.

In Ref. [83] solution (35) was used for the acoustic field calculation in an atmosphere stratified with respect to the density and sound velocity:

$$\rho(z)=\rho_0\exp\frac{z}{H}\,,\qquad c=c_0(1+kz)\,.$$

The plane $z=0$ is located at a height of 10 km, the z-axis is directed downward along the vertical; $H=8$ km, $k=1.3\times10^{-2}$ km^{-1}, $c_0=300$ m s^{-1}, $\rho_0=0.37$ kg m^{-3}. At $z=0$ the curved phase front was specified as well as the nonuniform amplitude distribution:

$$\psi_0(x=\alpha)=h\left(1+\frac{\alpha^2}{h^2}\right)^{1/2},\qquad A_0(\alpha)=p_0\left(1+\frac{\alpha^2}{h^2}\right)^{-1/2}, \tag{36}$$

where h is the height (over the plane $z=0$) at which lies the focus of a cylindrical diverging wave ($h<0$ corresponds to the converging wave), and α is the current abscissa value fixing the point of ray departure. The shock formation length was set at $l_s=2.3$ km corresponding, for example, to the N-pulse with characteristic duration $T_0=0.05$ s and peak pressure $p_0=180$ Pa.

In Fig. 9 is shown the ray pattern (28) for the diverging beam ($h=21.3$ km) as well as lines of equal levels of the peak pressure for a single pulse (Fig. 9a) and for a periodic 'saw' (Fig. 9b). As the distance traversed by the wave increases, the acoustic pressure decreases because of nonlinear absorption and divergence of rays.

Thereafter the wave penetrates into more dense atmospheric layers and the pressure is built up. As a result, the spatial distributions of peak pressure have a 'saddle' point; it is located for the pulse at a height of 5 km approximately, but for the periodic saw (which decays more strongly) at the distance 1 km from the Earth's surface.

The amplitude behaviour is determined by the joint action of refraction, the change in parameters of the medium along each ray, as well as by the nonlinear absorption. To select the influence of nonlinear absorption, let us consider the converging wave in a homogeneous medium, where Eqns (30) and (28) in terms of the first formula (36) take the form

$$D=\left(1-\frac{z}{h}\right)\left(1+\frac{\alpha^2}{h^2}\right)^{-1/2},\qquad x=\alpha\left(1-\frac{z}{h}\right). \tag{37}$$

The obvious point follows from Eqn (37) that the decrease in ray tube cross section that is proportional to D happens in homogeneous media only because of the divergence of the initial ray beam. The rays $x(z)$ remain straight lines in this process. On-axis peak pressure decreases at first because of nonlinear absorption, but thereafter it grows indefinitely as it approaches the focus. In contrast, the beam width increases because of strong absorption in the paraxial region. However, at the point $z = h$ the beams collapse and their width goes to zero.

The simplest phenomena described above have a primary effect on the complex pattern of the sawtooth wave field in an inhomogeneous medium.

5. Focusing of shock waves

To create strong wave fields, focusing devices can be used which have a wide application in many ultrasonic technologies and in medical instruments. A concentration of the wave energy occurs during the focusing, and the importance of nonlinear effects increases significantly. In addition, the linear dissipative properties of the medium are essential, but in the focal region the diffraction is of basic importance.

Let us consider, at first, the role of each of the indicated phenomena by itself. The solution of the linearised KZ equation (13) for Gaussian beams at the axis ($r = 0$) has the form [48, 52]

$$p = \int_{-\infty}^{\infty} \sin(\omega\tau + \varphi)\,\frac{\tilde{p}_0(\omega)\,\mathrm{d}\omega}{\left[(1 - x/x_0)^2 + x^2/x_d^2\right]^{1/2}}\,, \tag{38}$$

$$\varphi = \arctan\frac{x/x_d}{1 - x/x_0} + \pi\Theta(x - x_0)\,.$$

Here $x_d = \omega a^2/2c_0$ is the diffraction length (16), Θ is the Heaviside step-function, $\tilde{p}$ is the initial wave spectrum. At the geometric focus $x = x_0$ the solution (38) takes the form

$$p = \int_{-\infty}^{\infty} \frac{x_d}{x_0}\,\tilde{p}_0 \sin\left(\omega\tau + \frac{\pi}{2}\right)\mathrm{d}\omega = \frac{a^2}{2c_0 x_0}\,\frac{\partial}{\partial\tau}\int_{-\infty}^{\infty} \tilde{p}_0(\omega)\sin\omega\tau\,\mathrm{d}\omega\,. \tag{39}$$

Consequently, the profile at the focus is the time derivative of the initial (at $x = 0$) signal.

If the signal is a harmonic one, the maximum of its amplitude is achieved at the point $x_{\max} < x_0$ (which is located between source and geometric focus) and the maximum amplification factor is large, $K \gg 1$ (for weak influence of diffraction). According to Eqn (38) these quantities are

$$x_{\max} = \frac{x_0}{1 + x_0^2/x_d^2}\,, \quad K = \left(1 + \frac{x_d^2}{x_0^2}\right)^{1/2}\,. \tag{40}$$

In Ref. [84] the distortion process is described for a unipolar pulse signal $p = p_0\exp(-|\tau|/T_0)$. During the propagation a negative 'tail' appears owing to the diffraction. As the wave tends to the focus, the 'amplitude' increases for both compression and rarefaction phases, and the signal becomes differentiated with respect to time. Behind the focus these maxima decrease because of diffraction; the pulse profile tends to the form inverted relative to the initial one.

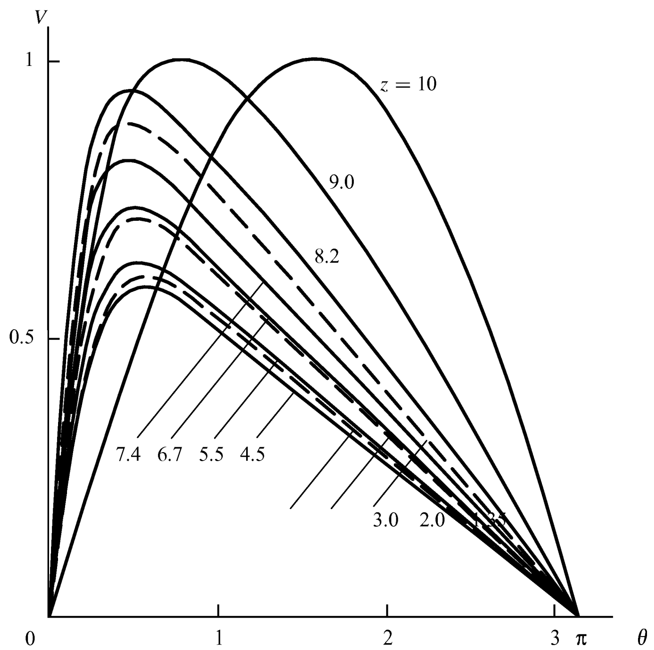

Figure 10. Distortion of the half-period of a spherical wave at its convergence to the focus. Number $\Gamma = 0.1$. The dimensionless distance $z = x/x_s$ from the current position of the front to the focus is indicated for the curves.

Let us neglect the diffraction now and consider the behaviour of a nonlinear spherically converging wave. The corresponding solution of Eqn (18) with an added dissipative term (or the modified Burgers' equation for converging waves [85]) written in dimensionless variables (17) has the form [31]

$$V = A(z)\left\{-\theta + \pi\tanh\left[\frac{\pi A(z)}{2\Gamma}\,\theta\right]\right\}\,, \tag{41}$$

$$A = \frac{z_0}{z}\left(1 + z_0\ln\frac{z_0}{z}\right)^{-1}\,. \tag{42}$$

The solution (41) describes, at small numbers $\Gamma = x_s/x_a$, one period $(-\pi < \theta < \pi)$ of the sawtooth wave. It was obtained for the signal harmonic at the source (at $x = x_0$ or $z = x_0/x_s = z_0$). The signal propagates to the centre $(x = z = 0)$ and the normalised distance decreases from z_0 to 0.

In Fig. 10 [31] one half-period is shown of the wave for $z_0 = 10$, in the case where the distance between the initial spherical surface and the focus exceeds the shock formation length significantly. In these conditions an interesting phenomenon can be observed — the double formation of the shock front [85, 31]. Fig. 10 shows the distortion of an initially ($z = z_0 = 10$) harmonic wave during propagation to the focus. In the curve $z = 8.2$ the steep leading front is clearly defined. Thereafter, the maximum disturbance decreases in the wave and its front expands — up to the curve $z = 4.5$. The shock front width reaches its maximum value at a point $z_{\max} = z_0\exp(1/z_0 - 1)$; in its vicinity the process of nonlinear absorption of the 'saw' is attenuated. However, at further approach closer to the focus, the disturbance starts to grow again (the convergence dominates over dissipation), and the front becomes steep again.

Evidently, nonlinear absorption of the 'saw' leads to a decrease in the amplification factor at the focus [5].

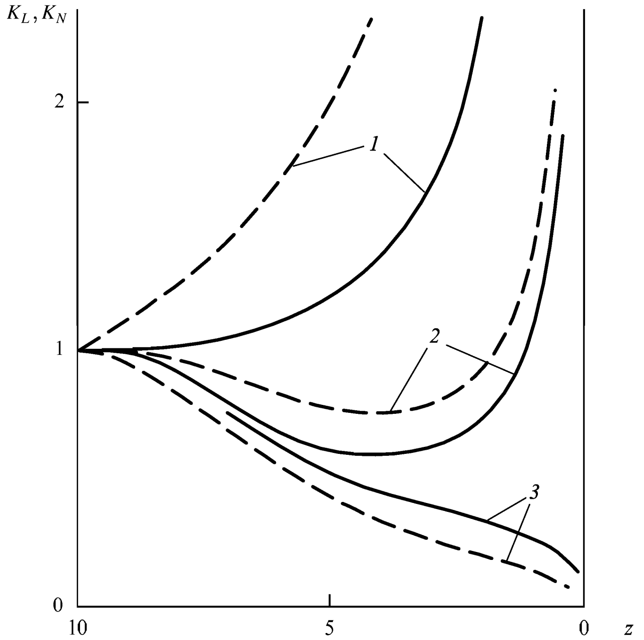

Figure 11. Change in linear (*1*) and nonlinear (*2*) amplification factors and their ratio (*3*) during the wave propagation from source ($z = 10$) to focus ($z = 0$): solid curves $\Gamma = 0.1$; dashed ones $\Gamma = 0$.

According to solution (41) the ratio between nonlinear K_N and linear K_L amplification factors is equal to

$$\frac{K_N}{K_L} = \frac{2\Gamma}{\pi}\,\frac{z}{z_0}\exp\left[\Gamma(z_0 - z)\right]$$
$$\times\left[y^{1/2}(y-1)^{1/2} - \operatorname{arccosh}\left(y^{1/2}\right)\right], \quad y = \frac{\pi A^2}{2\Gamma}, \tag{43}$$

where A is given by formula (42). The dependences of the amplification factors K_N, K_L, and their ratio (43) on z are presented in Fig. 11 (curves *1, 2, 3*, respectively). The dashed curves correspond to the vanishingly small dissipation, $\Gamma \to 0$, and solid curves to $\Gamma = 0.1$. The nonlinear amplification factor K_N has a minimum between the source and the focal point, where the wave front broadens (see Fig. 10). At the approach to the focus both factors K_N, K_L increase, but their ratio tends to zero (curves *3* in Fig. 11).

However, the nonlinear effects cannot only decrease the amplification factor, but increase it as well because of stronger focusing of higher harmonics generated by the intense wave [86, 73]. Such an inverse effect is possible in that case if nonlinear absorption cannot lead to marked energy losses in the whole path from the source to focal region, i. e. even though the 'saw' is formed, it happens in the immediate vicinity of the focus. The corresponding calculation is performed in Ref. [87] by the use of a step-by-step approach.

The wave was supposed, at the first stage of propagation in the region $x_0 > x > x_*$, to exhibit nonlinear distortion only, like a symmetric spherically converging wave [31]:

$$\frac{p}{p_0} = \frac{x_0}{x}\sin\left(\omega\tau + \frac{p}{p_0}\,\frac{x}{x_s}\ln\frac{x_0}{x}\right). \tag{44}$$

The stage boundary x_* can be chosen from compromise considerations. It must be small in comparison with the focal distance ($x \ll x_0$) but large with respect to the size of the focal region ($x_* \gg x_0^2/x_d$). At the second stage $x_* > x > 0$ the wave was supposed to exhibit only the diffraction transformation; here nonlinear distortion cannot be cumulative (because of the small size of the focal region), despite the large peak pressures and steepness of the shock front.

Using Eqn (44) as a boundary condition (at $x = x_*$) for the solution of the diffraction problem (39):

$$p\Big|_{x=0} = \frac{a_*^2}{2c_0 x_*}\left(\frac{\partial p}{\partial\tau}\right)_{x=x_*}, \quad a_* = a\,\frac{x_*}{x_0},$$
$$\left(\frac{\partial p}{\partial\tau}\right)_{\max} = \omega p_0\,\frac{x_0}{x_*}\left(1 - \frac{x_0}{x_s}\ln\frac{x_0}{x_*}\right)^{-1},$$

one can calculate the nonlinear amplification factor

$$\frac{K_N}{K_L} = \left(1 - \frac{x_0}{x_s}\ln\frac{x_0}{x_*}\right)^{-1}. \tag{45}$$

As can be seen, the greater the excess of K_N over K_L, the stronger is the nonlinearity (or smaller nonlinear length x_s); the dependence on the indefinite boundary x_* of this stage is weak. In experiments [88, 89] the increase of the focal field in comparison with the linear case was indicated. However, the principal question about the maximum possible ratio K_N/K_L is not yet understood. This is connected with difficulties in simultaneous consideration of the diffraction and dissipation phenomena under 'sharp' focusing conditions.

It has been possible to obtain the solution of the KZ equation only for small angles of wave front convergence [56], which can describe the nonlinear and diffraction evolution of the profile. This solution can be written in parametric form (21), where

$$f = \frac{Nz_0}{\sin\eta + Nz_0\cos\eta},$$
$$\eta = \pi\Theta(z - z_0) + \arctan\frac{Nz}{1 - z/z_0}. \tag{46}$$

Here the normalised distance $z = x/x_s$ varies through a range from $z = 0$ (the source) to increasing values of z. The geometric focus is located at $z = z_0 = x_0/x_s$.

The profiles constructed in accordance with solution (21), (46) are shown in Fig. 12. The increase in amplitude as well as leading front steepening were observed during propagation to the focus. Moreover, zero front level points of the wave profile are shifted in a forward direction, because of diffraction. The profile becomes asymmetric in geometric focus as a result of diffraction dephasing of harmonics; the positive pressure area is amplified more strongly. Just behind the focus (the curve for $x/x_0 = 1.2$ in Fig. 12) the profile takes a form similar to the derivative from the profile ahead of the focus (the curve for $x/x_0 = 0.8$). The ratio between nonlinear and linear amplification factors for the positive peak pressure in accordance with this solution is equal to

$$\frac{K_N}{K_L} = 1 + \frac{x_0}{2x_s}\,Q\left(y = \frac{x_0}{x_d}\right), \quad Q = \frac{(\pi/2)y - \ln y}{1 + y^2}. \tag{47}$$

Formula (47) is somewhat different from the result (45) of step-by-step analysis, but it shows the same qualitative dependence on x_0/x_s.

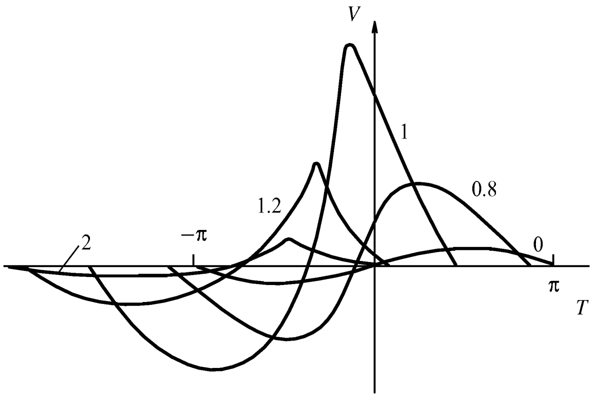

Figure 12. Distortion of the profile of an initially harmonic signal passing through the focus. Numbers at curves denote the dimensionless distance x/x_0 measured in units of focal length x_0. Diffraction ($x_d = 10x_0$) and nonlinearity ($x_s = 3.3x_0$) are significant.

Let us discuss now the phenomena which appear in the focusing process of nonlinear pulse signals containing shock fronts. Investigation of these problems in recent years was stimulated by medical applications and, most of all, by shock wave extracorporeal lithotripsy [18, 19]. Its purpose is the noncontact removal of kidney and gall stones from the human body. High-power acoustic pulses are generated outside the patient's body, then they become incident after focusing on the target calculus for fragmentation; the small fragments can be removed by natural processes. A significant number of papers at the recent international symposia on nonlinear acoustics, acoustical congresses and seminars was devoted (see, for example, Refs [16, 90–94]) to physical problems of power pulse generation, focusing, as well to the calculus disruption mechanism.

Three types of sources are used at present for the generation of intense pulses: electrohydraulic, electromagnetic and piezoelectric [19, 91]. Alternative sources are developed to improve the acoustic radiation characteristics and to diminish harmful side effects, for example, the detonation of very small explosive charges [94]. Optoacoustic generators [95] in which high-power pulses can be excited by absorption of modulated laser radiation [96–99], give considerable possibilities of controlling the pulse duration and time profile, as well as the directivity pattern.

There is no clear understanding of the causes of calculi fragmentation by such pulses. There exist experimental indications that the front surface of the target can be destroyed in the main by cavitation — because of high pressures developing at gas bubble collapse or by cumulative jets arising at the nonsymmetric compression of the bubble [92]. The rear surface can be destroyed by negative pressure caused by the reflection of the pulse front from the free surface into the sample (the spallation phenomenon) [100].

During the design of commercial lithotripters and measurements of the high-power focused pulse fields generated by lithotripters, interesting nonlinear phenomena were observed: self-refraction, saturation of the peak pressure in focus, growth in the size of the focal region, the shift of the constriction away from the source, and some others [101–103]. It was necessary to understand the nature of these phenomena and to develop a corresponding mathematical description. These purposes have stimulated new experimental and theoretical research.

Fig. 13 demonstrates the self-refraction process of the shock front. For comparison the spherical fronts are shown by dashed lines, corresponding to linear focusing; the finite size of the constriction is determined here by the diffraction, which is different for various components of the broadband spectrum of the signal.

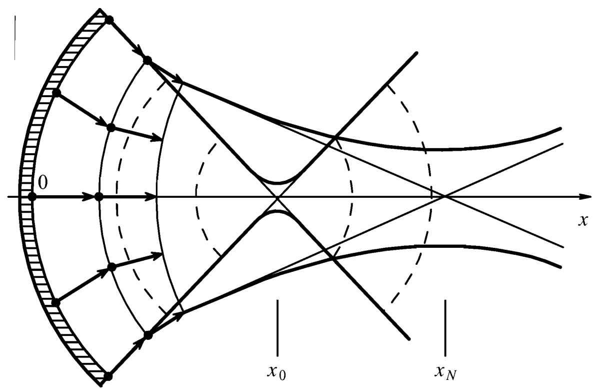

Figure 13. Self-refraction of a shock front leading to shift and broadening of the focal region.

Because the velocity of the weak shock wave $c = c_0\left[1 + \varepsilon A/(2c_0^2\rho_0)\right]$ depends on the pressure differential across the front, the transfer of the points lying in the front surface (marked by arrows) is greater near the axis than at a distance from it. There is simultaneously the process of nonlinear absorption, and the distribution of A over the front becomes more homogeneous (see Section 3). That slows down the self-refraction process. As shown in Fig. 13, the processes described above shift the nonlinear focus x_N with reference to the linear one x_0; the size of the nonlinear constriction is increased in this case.

These phenomena were observed in experiments [15, 104] as well, in which, moreover, the peak pulse pressures were measured at different distances from the source. A pulsed neodymium-glass laser was used for acoustic wave excitation. The laser was Q-switched and generated pulses of duration 30 ns at a wavelength 1.06 μm with energies 5–10 J. An optoacoustic converting cell of special design [95] was used which made it possible to generate acoustic pulses of 0.1–1 μs duration, peak pressure up to 1000 atm, and to form converging beams with diameter 50 mm and focal length 15–200 mm. The broadband receiving hydrophone on a base of piezoelectric film (PVDF) was calibrated and had a time resolution of order 10 ns, and space resolution of about 1 mm.

In Fig. 14a the dependences are presented of normalised pressure 'amplitude' A/p_0 on the distance x along the beam axis at different values of initial peak pressure p_0, equal to 9 atm (curves *1*), 100 atm (*2*) and 500 atm (*3*). Initial beam radius $a = 8$ mm. Dashed lines pass through experimental points.

One can see that marked amplification can be observed at small p_0 only (curve *1*). For the focusing of more power pulses the amplification was insignificant (curve *2*) or absent altogether (curve *3*). All the experimental points in the focal region lie below the solid curve *1*, which was calculated on the basis of linear theory; this indicates the marked effect of nonlinear phenomena. Theoretical dependences *2* and *3* (solid curves) were calculated with regard for

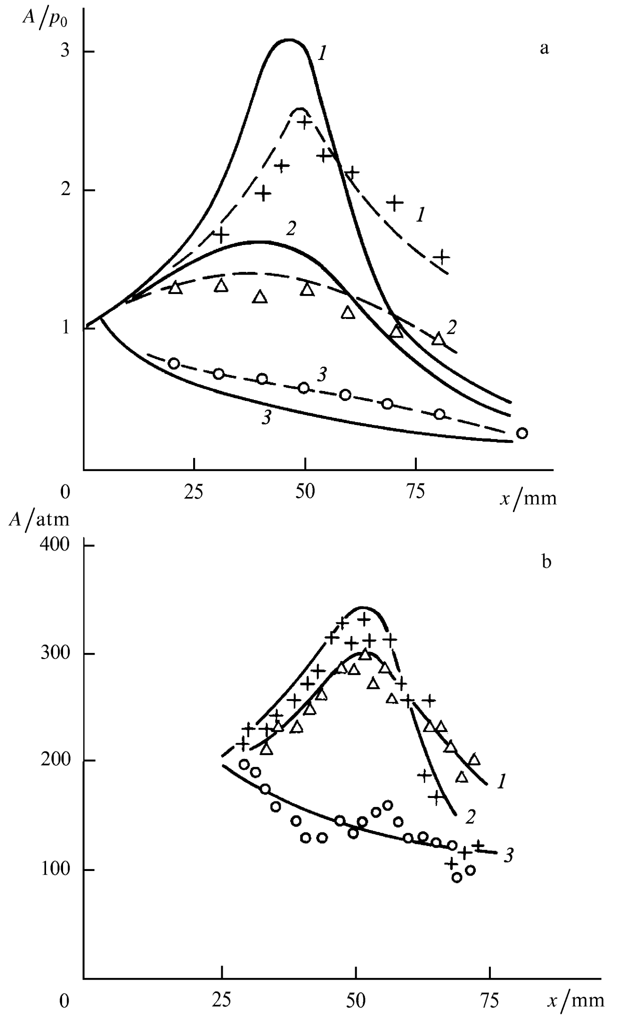

Figure 14. On-axis dependences of peak pressure at focusing of pulsed beams with different initial pressure (a) and different angles of convergence (b).

absorption and self-refraction [14, 105] to describe the experimental (dashed) curves *2* and *3*. In the theory the ratio $x_0/x_d = 2x_0 c_0 T_0/a^2$ between the focal length and the diffraction length was equal to 0.3, but the ratio of x_0 to the shock formation length $x_0/x_s = \varepsilon x_0 p_0/(c_0^3 \rho_0 T_0)$ for the curves *1, 2*, and *3* was 0, 3.2, or 16 respectively.

In Fig. 14b on-axis dependences of the peak pressure A are given for different angles of convergence $\varphi = 2\arcsin(a/x_0)$ equal to 32°, 22°, and 12° for the curves *1, 2*, and *3*. The initial amplitude $p_0 = 140$ atm ($x_0/x_s = 4.5$) was constant. The following values of the parameters a and x_0/x_d correspond to the curves *1–3*: 14 mm and 0.1, 10 mm and 0.18, and 5 mm and 0.75. By analogy with Fig. 14a, the peak pressure increase can be observed near the focus, but not in all cases. The effect is more clearly defined at larger angles φ: in curves *1, 2* the value of A exceeds p_0 significantly. In dependence *3* the pressure decreases with increase in x because of nonlinear absorption and self-refraction, and a local maximum appears only near the focus and is weakly expressed. So, one cannot reach marked amplification at small angles φ of wave front convergence.

To overcome the injurious effect of nonlinear processes it would be appropriate to use, firstly, pulses with a very gentle leading slope to inhibit shock-wave formation (from this time on, nonlinear absorption is in operation); secondly, it is necessary to use a strongly concave non-spherical transducer to compensate for refractional straightening of the wave front.

During our consideration of power focusing we have not yet addressed the transformation of the time profile of the signal passing through the focal region. These problems are extremely complicated and their solution can be obtained at present by numerical methods only [106, 107], even though the simplified model — the KZ equation — is used. The problem can be simplified radically in the special case that the strongly expressed self-refraction suppresses the diffraction distortions in the focal region (see Fig. 13). These cases are of great practical importance and can be analysed by modified methods (like nonlinear geometric acoustics), which use the different transport and eikonal equations for the description of smooth profile sections and, on the other hand, shock fronts [14, 105].

6. Nonlinear absorption and saturation

Nonlinear absorption which depends on the power of the disturbance (on amplitude, peak pressure and other parameters of this kind) is an important phenomenon of sawtooth wave physics whose significance was repeatedly underlined above. This phenomenon was studied intensively in the first works on nonlinear acoustics of condensed media (see reviews [3–5]), but recently here new results were obtained as well.

The peak values $A(x)/A_0$ in the plane waves shown in Fig. 1a–c decrease with the distance x according to the laws:

$$\left(1 + \frac{\varepsilon}{c_0^2}\,\omega A_0 x\right)^{-1}, \quad \left(1 + \frac{\varepsilon}{c_0^2 T_0}\,A_0 x\right)^{-1/2}, \quad \left(1 + c\gamma\omega A_0^2 x\right)^{-1/2}. \tag{48}$$

The absorptions (48) are different from the exponential one, typical for linear dissipative media, and depend on A_0 for quadratic nonlinear media [two first formulas (48)] or on A_0^2 for the media with cubic nonlinearity [the last formula (48) and (10)].

The absorption of sawtooth waves with an infinitely steep front does not depend on linear dissipative constants. It can easily be shown by means of Burgers' equation [1], which differs from Eqn (1) by the presence on its right side of the dissipative term $(b/2c_0^3\rho_0)\,\partial^2 u/\partial\tau^2$; it has just the same form as in Eqn (6). Let us consider for definiteness the periodic 'saw' in a quadratic nonlinear medium. Multiplying Burgers' equation by u and averaging over the period one can obtain

$$\frac{\partial \overline{u^2}}{\partial x} = -\frac{b}{c_0^3\rho_0}\,\overline{\left(\frac{\partial u}{\partial \tau}\right)^2}\,. \tag{49}$$

As can be seen from this equation, the decrease of mean intensity $I = c_0\rho_0\overline{u^2}/2$ with distance occurs more quickly for the presence of fronts having large values of the derivative $\partial u/\partial\tau$. For linear absorption of the harmonic wave $u = A(x)\sin\omega\tau$, where there are no steep sections in the profile, from Eqn (49) follows the usual law $A(x) = A_0\exp(-\alpha x)$ with the absorption coefficient $\alpha = b\omega^2/(2c_0^3\rho_0)$. For the sawtooth wave containing shocks of moderate width one can use the asymptotic (at $\Gamma \to 0$) solution (41) where $A(z)$ is given by the first formula (48). In this case the derivative squared in the right side of Eqn (49), $(\partial u/\partial \tau)^2 \sim b^{-2}$, is large for weakly absorbing media with small dissipation b. The shock front region with width $\sim b$ makes the dominant contribution to the integral which is to be calculated in averaging (49). Therefore, the dependence on b becomes weak and (49) takes the form

$$\frac{\partial \overline{u^2}}{\partial x} = -\frac{2\pi^2}{3}\frac{\varepsilon\omega}{c_0^2} A^3(x) + O(b \sim \Gamma) . \tag{50}$$

At vanishingly small dissipation ($b \to 0$) the right side of Eqn (50) retains only the nonlinear term.

In Fig. 15 are shown by long-short dashed lines the dependences of normalised mean intensity on the distance for an initially harmonic signal in a quadratic nonlinear medium. Each curve is denoted by the corresponding value of the number $\Gamma = x_s/x_a \sim b$. At $\Gamma = 0.01$ the dissipation is weak and considerable attenuation occurs over the region $z = x/x_s > 1$ only, after the steep front formation. With increase in Γ the fronts become more gentle and the relative contribution of linear absorption increases.

The excess nonlinear absorption calculated on the basis of curves for mean intensity,

$$\frac{\alpha_N - \alpha}{\alpha} = -\frac{1}{2\Gamma}\frac{\partial}{\partial z}\ln \overline{u^2} - 1 , \tag{51}$$

is shown by solid curves in Fig. 15. It is maximum at small Γ over that space region where steep fronts exist.

The partial absorption coefficients are often measured in experiments for different harmonics. For their calculation one has to use the spectral expansions of solutions (41) describing sawtooth waves, such as the Fay expansion [1]. In particular, for the first harmonic the expression [5]

$$\frac{\alpha_N - \alpha}{\alpha} = \exp\left[-\Gamma(1+z)\right]\sinh^{-1}\left[-\Gamma(1+z)\right] \tag{52}$$

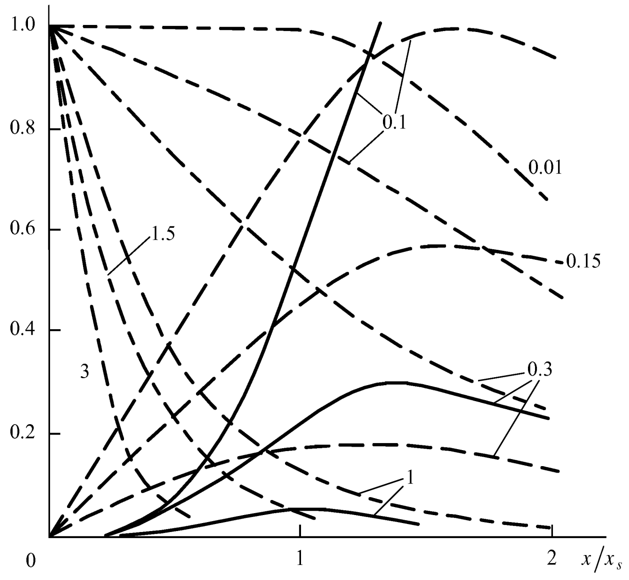

Figure 15. Dependences on distance of normalised mean intensity (long-short dashed lines) and excess nonlinear absorption (solid lines) at different numbers Γ. The excess absorption of the first harmonic is shown by dashed lines.

can be obtained. It is valid in the region $x > 3x_s$. At smaller distances ($0 < x < 2x_s$) the numerical data [31] are used for the construction of dashed curves in Fig. 15 ($\Gamma = 0.1$, 0.15, and 0.3). These curves indicate also that the most intensive absorption occurs in the small region of the front of the 'saw'.

In order to take into account not only the losses, but also energy injection into the wave, let us consider the inhomogeneous Burgers' equation [108]:

$$\frac{\partial u}{\partial x} - \frac{\varepsilon}{c_0^2}u\frac{\partial u}{\partial \tau} - \frac{b}{2c_0^3\rho_0}\frac{\partial^2 u}{\partial \tau^2} = Q . \tag{53}$$

The field Q of external sources can be created, for example, by heating the surface by moving a 'spot' of electromagnetic radiation [96] or by striction caused by two intersecting laser beams [109]. Let us take for definiteness that $Q = \partial(\beta T'/2)/\partial\tau$, created by thermoelastic stress $p = c_0^2\rho_0\beta T'$, where β is the thermal expansion coefficient, T' is the deviation of temperature. If T' varies with time accord- ing to the harmonic law, $Q = (p_0\omega/2c_0^2\rho_0)\sin\omega\tau$. It is convenient to write Eqn (53) in this case in dimensionless form:

$$\frac{\partial U}{\partial z} - U\frac{\partial U}{\partial \theta} - \frac{\partial^2 U}{\partial \theta^2} = A\sin\theta , \tag{54}$$

where

$$\theta = \omega\tau , \quad z = \frac{x}{x_a} = \frac{b\omega^2}{2c_0^3 p_0}x , \quad U = \frac{2\varepsilon c_0\rho_0}{b\omega}u ,$$

$$A = \frac{2\varepsilon p_0 c_0^2\rho_0}{b^2\omega^2} = \frac{\omega}{2c_0}\frac{x_a^2}{x_s} . \tag{55}$$

At small distances z traversed by the wave, its time profile $U \approx zA\sin\theta$ copies the profile of external sources. Nonlinear distortion may be amplified with increase in amplitude, and leads to the appearance of a shock front at each period of the wave. At $z \to \infty$ the stationary profile can be established [108]:

$$U = 2\frac{\partial}{\partial\theta}\ln \mathrm{ce}_0\left(\frac{\theta}{2}, A\right) , \qquad -\pi \leqslant \theta \leqslant \pi , \tag{56}$$

where ce_0 is the Matiew function. At $A \gg 1$ the stationary wave takes the form of a 'saw' with finite width of the front:

$$U = 2\sqrt{A}\left[\cos\frac{\theta}{2} + \tanh\left(A^{1/2}\theta\right) - 1\right] , \quad 0 \leqslant \theta < \pi . \tag{57}$$

Consequently, the nonstationary process goes on in the following way. The energy is introduced by sources into the whole region $-\pi \leqslant \theta \leqslant \pi$ of the period to be considered. Because of nonlinear distortion of the profile it tends to concentrate in the vicinity of $\theta = 0$, where the shock front exists. The stationary propagation regime is reached at the instant when the energy contribution from the source will be compensated by growing losses at the front. Mean intensity can be described by the equation

$$\frac{\partial \overline{U^2}}{\partial z} = -2\overline{\left(\frac{\partial U}{\partial \theta}\right)^2} + 2A\overline{U\sin\theta} . \tag{58}$$

It can easily be shown with the use of solution (57) that both terms in the right side of Eqn (58) are equal to $(8/3\pi)A^{3/2}$ but have different sign. So, there exists an energy balance. As this takes place, $\overline{U^2} = 2A = \mathrm{const}$.

Nonlinear absorption of sawtooth waves leads to the appearance of a saturation effect, in some cases. One can see from the first formula (48) that after several nonlinear distances $x_s = c_0^2/(\varepsilon\omega A_0)$ travelled by a wave in a quadratic medium, the peak particle velocity does not depend on its initial value A_0: $A_{\lim} = c_0^2/(\varepsilon\omega x)$. It means that in parallel with A_0 the nonlinear absorption increases as well, which weakens the dependence $A(A_0)$ at definite distance x. At $A_0 \to \infty$ the disturbance A no longer depends on A_0 and reaches its limiting value $A_{\lim}$.

Similarly, the trapezoidal 'saw' saturates in a cubic nonlinear medium [the third formula (48)]. In contrast to this, the unipolar pulse [the second formula (48)] does not saturate; at $x \gg x_s$ a slower (square root-like) dependence $A(A_0)$ takes over: $A = (c_0^2 T_0 A_0/\varepsilon x)^{1/2}$. So, by means of amplification of the initial pulse signal A_0, one can reach an amplification of the disturbance $A(x)$ in the medium as large as desired.

However, limiting values $A_{\lim}$ can be determined not only by nonlinear constants, but by dissipative properties of the medium as well. If at the input the harmonic signal is given and the inverse acoustic Reynolds number is $\Gamma \ll 1$, at distances $x \approx 2x_s$ the sawtooth wave can be formed and the saturation effect described above can be observed over the region where the 'saw' exists. At larger distances ($x \approx 2x_a$), because of the joint action of nonlinear absorption and dissipative smoothening, the wave transforms again to a harmonic wave, the amplitude of which does not depend on its initial value A_0 [1]. So, the limiting fields can be described within one period ($-\pi \leqslant \omega\tau \leqslant \pi$) by formulas

$$u_{\lim} = \frac{c_0^2}{\varepsilon\omega x}\left[-\omega\tau + \pi\,\mathrm{sign}\,(\omega\tau)\right], \qquad 2x_s < x < x_a ,$$

$$u_{\lim} = \frac{2b\omega}{\varepsilon c_0 \rho_0}\exp\left(-\frac{x}{x_a}\right)\sin\omega\tau, \qquad x > 2x_a . \tag{59}$$

It can easily be shown using (59) that even in water, which is a weakly dissipative medium, the intensity of an ultrasonic wave with the frequency 4 MHz at the distance 1 m cannot exceed 0.2 W cm^{-2} and at the distance 5 m, 10^{-3} W cm^{-2}.

It is impossible to transport the high densities of ultrasonic energies through large distances into dispersionless media. This fact sets the restrictions on the possibilities of force and energy action of such waves through a distance.

One way to decrease nonlinear losses connected with shock front formation was suggested in Ref. [110]. This method is based on the following idea. The steep front is formed by higher harmonics resulting from cascade-like nonlinear processes which take place with the obligatory participation of the second harmonic. If the spectrum is free from the frequency 2ω, the channel of energy flow will be closed in the direction of high frequencies ($\omega \to 2\omega \to 3\omega \to \ldots$). To remove the harmonic 2ω from the coherent component of the wave field, it is possible to introduce into the medium selectively absorbing or scattering objects (like one-size gas bubbles, narrow band filters, etc.). But we have no prior knowledge of the influence of this action on the fundamental frequency wave ω: will it decay more slowly or will the new channel of energy losses ($\omega \to 2\omega$ and then to heat or to the scattered field) replace the previous energy stream upward over the spectrum?

To calculate the wave profile in the nonlinear medium containing elements selectively absorbing the frequency 2ω, it is necessary to solve the integrodifferential equation [110]:

$$\frac{\partial V}{\partial z} - V\frac{\partial V}{\partial\theta} - \Gamma\frac{\partial^2 V}{\partial\theta^2} = -DB_2(z)\sin 2\theta , \tag{60}$$

$$B_2 = \frac{2}{\pi}\int_0^{\pi} V(z,\theta)\sin 2\theta\,\mathrm{d}\theta .$$

Here D is the coefficient of additional absorption caused by selectively absorbing elements, and B_2 is the second harmonic amplitude. In the form (60), normalised variables (17) are used.

The dependences of the amplitudes of harmonics ω and 2ω on the distance [111] show that with increase in selective absorption D the second harmonic is generated less effectively. In addition, the first harmonic amplitude decrease occurs more slowly with increase in z, than in the absence of absorption at the frequency 2ω ($D = 0$). Even at $D > 4$ the profile remains smooth over a length of several x_s. The shock fronts do not appear and nonlinear absorption is damped.

This phenomenon was studied experimentally [112]. At one end of the open acoustic resonator an ultrasonic source was placed, the resonant frequency of which could be varied in the vicinity of 1 MHz. The mirror placed at the other end could be totally reflecting or could partially transmit the wave with frequency 2ω (up to 40% in amplitude). Losses for the second harmonic frequency were created artificially by means of a selectively transmitting mirror. It turned out that the Q-factor increased more than two times if the nonlinear resonator had selective losses. So, calculations and experiments [110–112] showed a surprising, at first sight, fact: the insertion of dissipative elements into the medium leads to the reduction of losses.

The discussion up till now has been based upon plane sawtooth waves, formed as a result of nonlinear distortion of a signal, harmonic at the input to the medium. For one-dimensional converging or diverging waves (spherical and cylindrical) the saturation will be observed as before but the rate of the nonlinear processes will be different [31].

The radically new behaviour can be demonstrated by a unipolar pulse propagating as a focused beam. As was mentioned above the peak pulse disturbance [second formula (48)] does not saturate. However, it was shown in Section 5 that self-refraction and nonlinear absorption lead to the decrease of the amplification factor during focusing, as well as to broadening of the focal region (see Figs 13 and 14). These are precisely the effects which limit the maximum pressure that can be obtained in the focus of high-power pulse concentrators. The limiting pressure is defined by the characteristic internal pressure of the medium $p_* = c_0^2\rho_0/2\varepsilon$ as well as by the angle of convergence $\beta = a/x_0$ at the focus. For Gaussian beams with an initially spherical front a theoretical evaluation [14, 100] was obtained:

$$p_{\lim} \approx 1.5 p_* \beta^2 . \tag{61}$$

For water and angles of convergence $\beta = \pi/6$ the limiting pressure in accordance with (61) is approximately equal to 1300 atm. This value is near to experimental data [102] obtained in the process of measurements performed in the field of commercial lithotripters. The limiting pressure depends, of course, on the shape of the focusing surface as well as on the initial field distribution over it. These reasons will influence the coefficient in formula (61).

7. Kinetics of sawtooth-shaped waves

It is helpful to use the analogy between an ensemble of weak shock waves (Fig. 16) and a gas of perfectly inelastic particles. Let us consider a single 'step' with finite width of the front. Its evolution in a dissipative quadratically-nonlinear medium is described by the solution of Burgers' equation [1, 113]:

$$u = \frac{u_{i+1}+u_i}{2} + \frac{u_{i+1}-u_i}{2}\tanh\left[\frac{\varepsilon c_0 \rho_0}{b}\,\frac{u_{i+1}-u_i}{2}\left(\tau + \frac{\varepsilon}{c_0^2}\,\frac{u_{i+1}+u_i}{2}\,x\right)\right]. \quad (62)$$

Here u_i and u_{i+1} are particle velocity values just before and behind the shock front. We associate the height of each 'step' $(u_{i+1}-u_i)$ with the mass m_i of a particle correlated with the step, and we associate the rate of displacement of the front in the accompanying coordinate system $(\tau = t - x/c_0)$ with the velocity v_i of that particle. According to formula (62), the motion of the front obeys the law:

$$v_i = \frac{d\tau_i}{dx} = -\frac{\varepsilon}{2c_0^2}(u_{i+1}+u_i)\ . \quad (63)$$

Velocity (63) increases with increase in number i. Therefore, the succeeding front $(i+1)$ will overtake the preceding one (i). They merge together, and the mass and momentum of the associated particles are conserved in the collision:

$$m_i' = m_i + m_{i+1}\,, \qquad m_i' v_i' = m_i v_i + m_{i+1} v_{i+1}\ . \quad (64)$$

The wave–particle analogy will be more illuminating if we consider the wave of acceleration instead of the wave of velocity:

$$\frac{\partial u}{\partial \tau} = D\cosh^{-2}\left[\left(\frac{\varepsilon c_0 \rho_0}{b}\,D\right)^{1/2}(\tau + x v_i)\right]\ . \quad (65)$$

The expression (65) resembles the soliton solution of the Korteveg–de Vriese equation (Fig. 16b). As for a soliton, the duration of this pulse disturbance decreases with increase in its 'amplitude' $D = (\varepsilon c_0 \rho_0/4b)(u_{i+1}-u_i)^2$ according to $D^{-1/2}$. But the velocity v_i (63) does not depend on D; in accordance with solution (62) it is determined not by the 'jump' differential $(u_{i+1}-u_i)$, but by the mean value of the disturbance $(u_{i+1}+u_i)/2$ at the front. And, finally, there exists a principal distinction: the solitons collide with one another like perfectly elastic particles (see, for example, [48]), but single pulses (65) collide like absolutely inelastic ones.

The sequence of several 'steps', shown in Fig. 16, can be achieved, for example, in experiments using shock tubes. But there exists a more typical disturbance having the form of a sawtooth wave with different and randomly disposed shocks. Such a wave is interesting for the description of characteristics of one-dimensional acoustic turbulence [114–116]; it forms during the evolution of the profile of broadband noise waves travelling through nonlinear weakly dissipative media. As distinct from 'steps' (Fig. 16), there is a decrease of 'teeth' (during time intervals between collisions) because of nonlinear dissipation of energy at fronts. This decrease can be considered as 'evaporation' of particles. Thus, the propagation of a random sawtooth wave can be regarded as a one-dimensional flow of 'evaporating' particles, which move with random velocities relative to the flow (its velocity is equal to c_0) and collide perfectly inelastically with one other.

Both types of statistical ensembles — 'steps' (Fig. 16) and 'teeth' — can be described by kinetic equations. Let us introduce the distribution function $g(x, t, m)$, which is the density function of the probability that time t has elapsed between two neighbouring discontinuities and that the height of the second one is equal to m. The evolution of the function g is a result of the free motion of the discontinuities in accordance with Eqn (63) and as result of their pair collisions.

The kinetic equation (of the Boltzmann equation type) for the ensemble of 'steps' has the form [117]

$$\frac{\partial g}{\partial x} - \frac{\varepsilon}{2c_0^2}\big(m + \langle m\rangle\big)\frac{\partial g}{\partial t} = \frac{\varepsilon}{2c_0^2}\left[m\int_0^m g(x,\,t,\,\xi)\times g(x,\,0,\,m-\xi)\,d\xi - \big(m - \langle m\rangle\big)g\int_0^\infty g(x,\,0,\,\xi)\,d\xi\right]\ . \quad (66)$$

The quadratically-nonlinear right-hand side of Eqn (66) is responsible for the inelastic pair collisions.

An analogous equation for the ensemble of 'teeth' [118] takes into account the nonlinear absorption of shocks (or 'evaporation' of particles), as well as the change in the slope of smoothed sections of the profile. It differs from Eqn (66) in the presence of additional terms in the left part of the kinetic equation which describe the probability of transport without collisions.

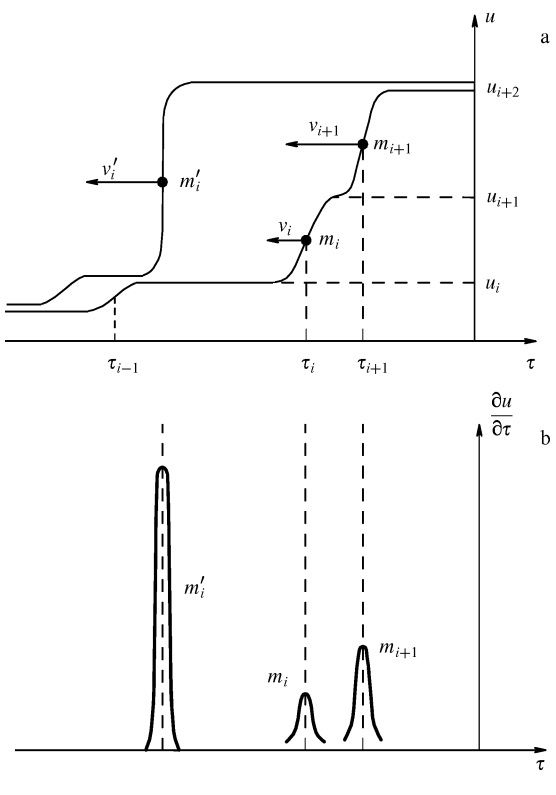

Figure 16. Merging of two weak shock waves together (a) and the analogy with inelastic collision of particles (b).

The normalisation condition obviously holds for a distribution function g that satisfies Eqn (66). If the function g is known, statistical averaging can be performed by the usual technique:

$$\langle \Phi \rangle = \int\int_0^{\infty} \Phi(x,\, t,\, m)\, g(x,\, t,\, m)\,\mathrm{d}t\,\mathrm{d}m\ . \tag{67}$$

In Ref. [117] exact and approximate solutions for the kinetic Eqn (66) were obtained and first integrals were derived. One of the exact solutions corresponds to the Poisson process. Introducing the new function $f(x,m)$ and its Laplace transform $\tilde{f}(x,s)$ according to the formulas

$$g = \frac{1}{t_0}\exp\left(-\frac{t}{t_0} - \frac{\varepsilon x}{c_0^2 t_0}\, m\right) f, \quad \tilde{f} = \int_0^{\infty} f \exp(-sm)\,\mathrm{d}m\ , \tag{68}$$

we obtain an equation of the Riemann-wave type,

$$\frac{\partial \tilde{f}}{\partial x} + \frac{\varepsilon}{c_0^2 t_0}\,\tilde{f}\,\frac{\partial \tilde{f}}{\partial s} = 0\ . \tag{69}$$

The solution of Eqn (69) is given by the implicit function whose form is determined by the initial (at $x = 0$) distribution:

$$\tilde{f} = \Phi\left(s - \frac{\varepsilon x}{c_0^2 t_0}\,\tilde{f}\right), \quad \Phi(s) = \int_0^{\infty} f(x=0,\, m)\exp(-sm)\,\mathrm{d}m\ . \tag{70}$$

In an analogous way the kinetic equation describing the ensemble of 'teeth' of a random sawtooth-shaped wave [118] can be solved.

In Fig. 17 the typical processes are shown — the transformation of exponential (a) and delta-shaped (b) initial distributions of masses $g(x,m)$. The normalised distance $z = \varepsilon\langle m\rangle x/(c_0^2 t_0)$ traversed by the wave is indicated for each curve. As is seen from Fig. 17b the collisions of discontinuities lead to the formation of fronts with double ($n = 2$), triple ($n = 3$) or higher multiples of amplitude. They are represented by line segments of appropriate height, the tops of which for n equal to 1, 2 and 3 at the given z are joined by dashed curves. Simultaneously, the amplitude of each front decreases by the factor $(1+z)^{-1}$ as a result of nonlinear absorption.

The main trends in the transformation of the distribution functions (Fig. 17) are an increase of the probability density function for large and small values of $\mu = m/\langle m\rangle$ and a decrease of the probability in the middle part of the distribution. The increase in the probability of small μ is attributable to nonlinear energy losses at the discontinuities. The main contribution here is from the segments of the case where the field decreases in the mean, and collisions are infrequent. The growth of the density function g at large values of μ is attributable to the merging of discontinuities and the formation of cumulative-amplitude fronts. The competition of these two trends leads to the appearance of the self-similar asymptotic, which for the Poisson process has the form

$$g \propto z^{-1/2}\mu^{-3/2}\exp\left(-\frac{\mu}{4z}\right)\ .$$

In this case the mean $\langle\mu\rangle$ remains constant but the variance $\langle\mu^2\rangle$ increases linearly with the distance travelled by the wave.

The spectral characteristics of one-dimensional acoustic turbulence can also be calculated with the use of the distribution function g and a solution of (62) type taking into account the finite width of the shock front. In particular, for the intensity spectrum of the Poisson process the following formula [118] can be obtained:

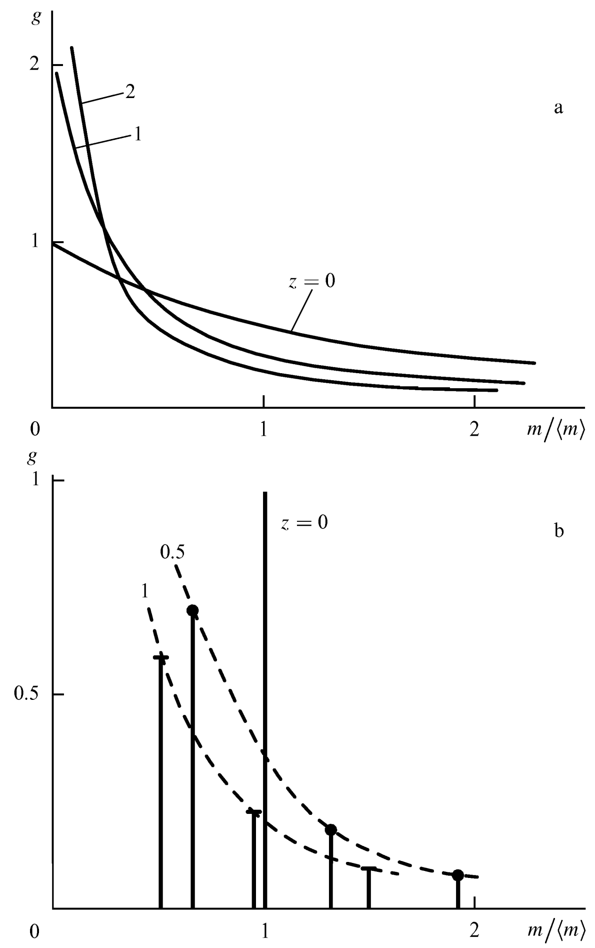

Figure 17. Transformation of probability distributions of 'jumps' of disturbance across discontinuities in a travelling sawtooth wave for exponential (a) and delta-shaped (b) distributions of linear sections of the profile of a sawtooth wave.

$$G(\omega) = \frac{2\pi^3\Gamma^2}{1+z}\int_0^{\infty}\frac{g(z,\,\mu)\,\mathrm{d}\mu}{\sinh^2(\pi\Gamma\omega t_0/\mu)}\ , \tag{71}$$

where $\Gamma = \varepsilon c_0\rho_0\langle m\rangle t_0/b$. To illustrate the peculiarities in the behaviour of the spectrum let us discuss the result obtained by averaging formula (71) where g is a self-similar distribution. It is readily shown that two characteristic intervals are discernible in the spectrum. In the frequency range $\omega t_0 \ll (\pi\Gamma)^{-1}$, as in the case of regular waves, the universal relation $G \propto \omega^{-2}$ is associated with the discontinuous parts of the profile. In the range $\omega t_0 \gg (\pi\Gamma)^{-1}$ the asymptotic form is $G \propto \exp\left[-(\omega z)^{1/2}\right] z^{-3/2}\omega^{-1/2}$; it decreases with the growth of frequency more slowly than for a regular sawtooth wave (see Ref. [119] also) where $G \propto \exp(-2\Gamma\omega t_0 z)$ [1].

The behaviour of spectra of nonlinear nondispersive waves (not only the sawtooth-shaped ones) was studied earlier without the use of the kinetic approach described above; the corresponding results are discussed in detail in works [20, 120] on statistical nonlinear acoustics.

8. On the interaction and self-action of waves containing shock fronts

A great quantity of investigation is devoted to the effects of wave interactions in media without dispersion; they are presented partly in monographs [1, 4, 6, 31, 52, 73, 120]. Over the years the interesting phenomena like self-demodulation, scattering of sound by sound, the excess absorption of the signal because of interaction with the external (in particular, noise) field, and many others have been observed and studied. Much attention was given to the nonlinear generation of low (difference) frequencies in the field of a modulated high-frequency pump wave. It is known that low frequencies can be radiated by the same space region where interaction occurs and they can propagate as a directed weakly absorbing beam over large distances; these features are used in parametric hydroacoustic systems [52].

However, only a few of these works contain information on sawtooth wave interaction. To study these processes, computer methods have been increasingly used in recent years. So, to solve diverse problems on weakly dispersive wave interaction, the universal application package NACSI [121] (Nonlinear Acoustics — Computer Simulation) was created. With the help of it one can calculate profiles and spectra of strongly distorted waves and wave beams, the propagation of which is described by evolution equations like the Burgers', KZ, Whitham and their modified forms for media with diverse dispersive and dissipative properties. For the numerical solution of such equations the problem is to reach high accuracy both for discontinuous regions (shock waves and contact shocks) and for smoothed sections of the profile. To do this one has to eliminate the known imperfections of classical algorithms leading to parasitic oscillations near fronts (without introduction of significant viscosity), to nonlinear instabilities and errors in calculation of smoothed parts caused by 'numerical scattering' — the influence of high gradients of the field. To eliminate the difficulties mentioned above the new 'shock trapping' codes were worked out in recent years, so-called 'high resolution' numerical schemes. Their basic properties are: the order of accuracy for calculation of the smooth part of the solution must be lower than second, and there should be a possibility to calculate shocks without fictitious oscillations. In addition, contrary to classical algorithms of second and higher order, they do not require artificial viscosity to be set in advance.

By means of the package NACSI the problems of interaction of plane, spherical and cylindrical (diverging and converging) waves, of diffracting and focused beams, as well as of disturbances propagating in a waveguide, horn, concentrator and ray tube can be solved effectively if the geometric acoustics approximation is used (see Section 4).

The initial profile can be a single pulse of arbitrary shape or a sequence of several different pulses (if their interaction is studied). The profile can be specified also as a sum of several (up to ten) harmonics with arbitrary amplitudes, phases and frequencies or can be given by piece-linear approximation. To obtain the results shown, for example, in Figs 4, 5 or 10, one needs personal computer operation time of the order of one minute.

Numerical methods for the study of sawtooth wave interaction are now in progress based on the use of known asymptotic formulas.

In solving complicated problems the computing time can be reduced significantly if combined approaches are used, comprising the direct integration of the equation by a difference algorithm and fast calculation on the basis of available asymptotics. There exists another way to improve algorithms based on the more complete use of prior knowledge of the wave process. So, the shocked wave calculation using the spectral approach necessitates solution of the system of coupled equations written for complex amplitudes of harmonic components of order $10^2 - 10^3$. However, it is known in advance, that the high-frequency wing of the spectrum is formed by synchronised harmonics whose amplitudes decrease according to the law ω^{-1}. Therefore the amplitudes and phases of higher harmonics can be calculated on the basis of simple algebraic formulas connecting these quantities with numerical data obtained for the several first (10^1) order spectral components [122]. In this case the calculation time can be reduced by $1-2$ orders.

Consequently, the sawtooth wave interactions are diverse, but results obtained there are basically numerical. As a consequence, only the principal or general properties of such phenomena will be discussed below.

Let us consider first the interaction between weak disturbances with both smooth and shocked parts of the sawtooth profiles. Let V_0 be a form of plane 'saw' and its disturbance V_1. Then from the homogeneous Burgers' equation [see Eqn (60), $D = 0$] the following can be obtained:

$$\frac{\partial V_1}{\partial z} - \frac{\partial}{\partial \theta}(V_0 V_1) = \Gamma \frac{\partial^2 V_1}{\partial \theta^2} . \tag{72}$$

For the sections of 'saw' linear in time $V_0 = (\theta_0 - \theta)/(z_0 + z)$ and the solution takes the form

$$V_1 = \left[4\pi\Gamma z\left(1 + \frac{z}{z_0}\right)\right]^{-1/2} \times \int_{-\infty}^{\infty} \exp\left[-\frac{1 + z/z_0}{4\Gamma z}\left(\frac{\theta - \theta_0}{1 + z/z_0} - t\right)^2\right] V_0(t)\,\mathrm{d}t\,. \tag{73}$$

In Fig. 18 one-half period of the 'saw' $V_0 = (\pi - \theta)/(1 + z)$, $0 < \theta \leqslant \pi$ is shown by dashed straight lines. The peak value for the shock which is placed at the point $\theta = 0$ decreases with increase of distance z equal to 0, 0.3, 0.8, 1.5. The behaviour of the harmonic initial disturbance $V_1(0, \theta) = m \sin 6\theta$, $m \ll 1$ is calculated in accordance with formula (73) for the same distances z in the absence of dissipation ($\Gamma = 0$). It is seen that both amplitude and frequency decrease as $(1 + z)^{-1}$. The inverse process is possible also: signal amplification and increase in frequency at the steepening leading front [123, 20] appearing in the 'saw' formation (in Fig. 18 it is not shown); it corresponds to values $z_0 < 0$ in solution (73). The varying of the signal frequency during interaction with sections of the 'saw' which were linear in time was observed experimentally [124, 125].

So, the transformation of the profile of the intense 'saw' is responsible for the harmonic disturbance 'flowing' to the front from both sides of it (see Fig. 18) and disappearing on the front because of nonlinear absorption (see Section 6).

To investigate the behaviour of disturbances in the vicinity of the shock, let us put in Eqn (72) $V_0 = \tanh(\theta/2\Gamma)$. This function describes the internal structure of the weak shock front. It is convenient to

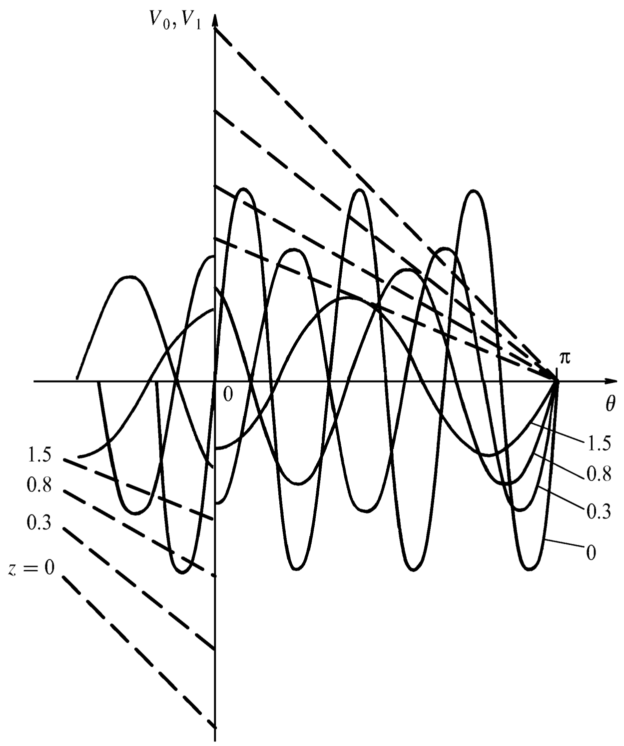

Figure 18. Evolution of harmonic disturbance of linear sections of the profile of a sawtooth wave.

write the solution of the resulting equation in terms of displacement S, where the velocity can be expressed as $V_1 = \partial S/\partial\theta$:

$$S = \frac{\exp(-z/4\Gamma)}{(4\pi\Gamma z)^{1/2}\cosh(\theta/2\Gamma)} \times \int_{-\infty}^{\infty} \exp\left[-\frac{(\theta-t)^2}{4\Gamma z}\right] \cosh\left(\frac{t}{2\Gamma}\right) S_0(t)\,\mathrm{d}t\,. \quad (74)$$

As the result (74) suggests, the initial disturbance (see Fig. 18) will be concentrated near the front and absorbed on it.

The evolution pattern of the interaction between disturbances and sawtooth waves, which is illustrated by Fig. 18 and solution (74), can be broken down with increase in the wave intensity. The self-reflection effect can be observed [1]: the wave ceases to be a wave travelling in one direction, after the shocks appear. The entropy undergoes a small jump in the transition through the shock front [63]. That jump is a weak inhomogeneity in the wave profile. The smooth portions of the profile, incident on the discontinuity, interact with it. This interaction leads to the appearance of reflected waves which propagate in the opposite (relative to the initial wave) direction. In the periodic 'saw' each discontinuity can be regarded as a 'generator' of reflected signals. Therefore, an overall effect caused by the summation of these signals can be significant and can lead, for example, to the appearance of acoustic wind [1].

The experimental observation of the self-reflection phenomenon [126] was performed in the radio-frequency range using a model of a nonlinear dispersionless medium: a long transmitting line of the low-pass filter type. A short radio pulse was radiated, and shock fronts appeared in it at the distance x_s. From this time on, a backward wave was beginning to be generated. That reflected wave was received at the input of the line with a time delay $2x_s/c$ (here c is the signal propagation velocity). In recent years there have appeared new works [127, 128] devoted to the self-reflection of sawtooth waves.

Let us pass now to the interactions of waves intersecting each other at an angle. It is known [1] that out of the intersection region of two intense beams with frequencies ω_1 and ω_2, only the weak signal of the combination frequency $\omega_1 \pm \omega_2$ can be measured. This is because it is impossible to organise the synchronous interaction between noncollinear waves in media without dispersion or, in other words, with the absence of the effect of resonant scattering of sound by sound. [129].

The solution of the problem obtained by successive approximation methods shows that nonlinearity generates two kinds of disturbances whose behaviour in space is essentially different. Along the direction of propagation of each beam harmonics are excited, the amplitudes of which increase with increase in traversed distance. In contrast to this, the harmonics observed in other directions oscillate in space and remain weak in comparison with the initial waves. Averaging the equations over the fast periodic oscillations, it is possible to show [130] that the superposition principle is valid approximately for signals periodic in time. So, nonlinear waves undergo self-action and their form can be distorted strongly, but intersection of such waves does not give birth to the appearance of intense scattered signals.

Nonsynchronous disturbances are small in comparison with the amplitudes of synchronously excited waves, if the angle of intersection is $\beta > (\varepsilon \mathrm{M})^{1/2}$, where ε is the nonlinearity of the medium, and M is the acoustic Mach number. For typical conditions, for example, when ultrasonic waves with intensities $1-10$ W cm $^{-1}$ are interacting in water, the amplitudes of nonresonant disturbances are negligible for angles of intersection $\beta > 4°$.

The idea of the superposition of two strongly distorted waves travelling in opposite directions was used in Ref. [130] to represent standing waves in a resonator with rigid walls. The discontinuous vibrations were shown to appear in the resonator after the opposed waves took the sawtooth-shaped form. The Q-factor decreases significantly in this case because of nonlinear absorption. The field is no longer a standing wave; a front of velocity disturbance appears moving between two walls. There can be several fronts of such a type ('travelling nodes') for higher vibration modes. In Ref. [130] forced vibrations excited by the distributed external force were analysed; they were represented as a sum of two opposed waves described by the inhomogeneous Burgers' equation (53).

In Refs [131 – 133] vibrations were considered in a resonator excited at one end by a periodic force; here the formation of a shocked field was also observed, which can be presented as a superposition of opposed waves.

Further development of these ideas is given in Refs [134, 135]. It was found to be possible to take into account the impedance character of boundaries and their movement [135]. If these vary the wave form weakly over time intervals of the order of the wave propagation time through the resonator, the field can be presented as the sum of two opposed travelling waves interacting with each other at the boundaries only.

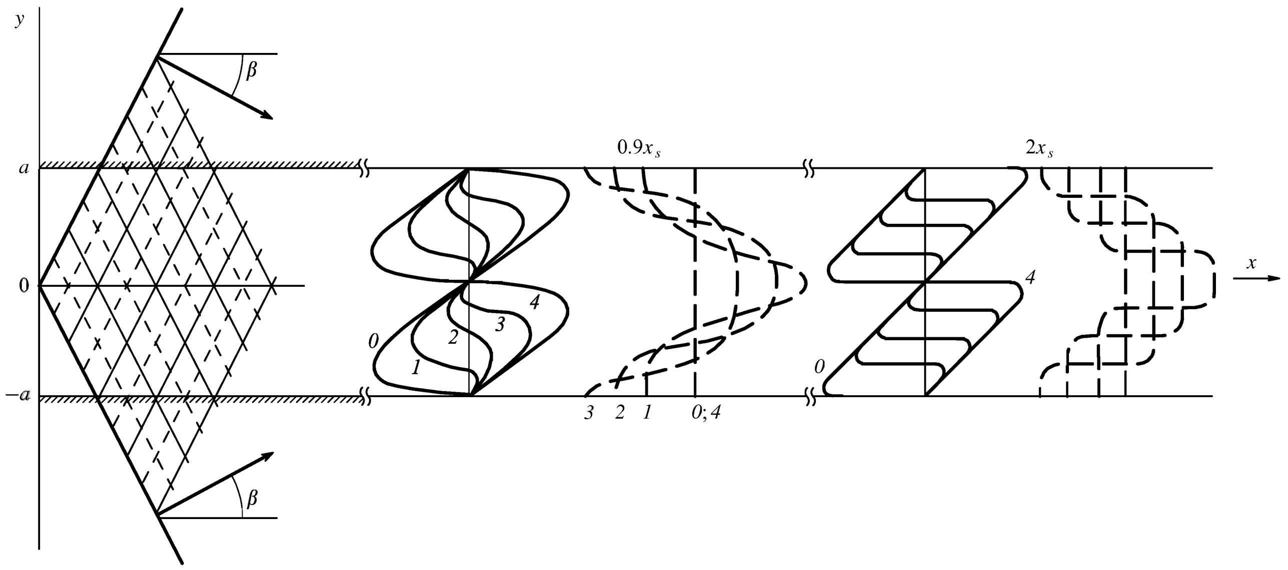

Figure 19. Formation of a mode by superposition of nonlinear waves travelling at equal angles to the waveguide axis.

Let us pass now from resonators to waveguide systems. It is known [48] that normal waves in a linear layer may be represented as a segment of an interference pattern formed by two harmonic waves of equal frequency propagating at angles $\pm\beta$ to the x axis (Fig. 19). Here in the nodal planes (for example, $y = \pm a$) two absolutely rigid waveguide walls may be placed without disrupting the motion pattern. The width $2a$ of such a waveguide is associated with the wavelength by the relationship $2a \sin\beta = n\lambda/2$. For intense waves it is possible to use the analogous treatment of normal nonlinear waves in a waveguide as a sum of two plane nonlinear waves which are periodic in time and travel at angles $\pm\beta$ with respect to the waveguide axis [136].

In Fig. 19 the distributions are shown for longitudinal u_x (solid curves) and transverse u_y (dashed curves) velocity components in different cross-sections of a waveguide, corresponding to the distances before $(x = 0.9x_s)$ and after $(x = 2x_s)$ the formation of a 'saw'. The curves are drawn for the second mode $(n = 2)$ at regular time intervals (curves *0–4*) $\Delta t = T/8$ within one-half of the period T. Large gradients of the velocity u_x appear near the axis of a waveguide and at its walls; the space distribution over a cross section has the 'sawtooth' form with two additional 'travelling nodes'. The lines of equal stream function, representing the pattern of particle velocities, become discontinuous [136]; there occur zones where there is strong nonlinear absorption.

The study of intense acoustic and shock waves propagating in waveguides, tubes, jet flows, etc., is of great practical importance [137]. When the wave is excited in a volume bounded by walls, it is possible to avoid diffraction losses and improve the observing conditions for nonlinear effects. Therefore, gas-filled and liquid-filled tubes are used often in experiments at high sound pressure levels [138–141]. The mode structure of the field is insignificant in many experiments, because long waves are used, as compared with the size of the cross-section.

In Ref. [142] the propagation of a high-frequency intense wave was studied in a round tube with rigid walls. The system of equations was solved for the longitudinal and transverse components of the particle velocity. That system was derived at the same approximation as the KZ equation (18). The tube axis was coincident with the axis of the beam. It turned out that unlike the case of an unbounded medium, the wave intensity oscillated along the axis with a space period of the order of the diffraction length x_d (16). Such behaviour is connected with the multiple reflections from the tube walls of the waves, forming the beam. At distances equal to 3–5 times x_d the intensity is distributed uniformly over the cross section due to diffusion 'smoothing' and the influence of walls; on further propagation the wave behaves like a plane one.

The wave form shows interesting behaviour. In Fig. 20 the dependences are given of the longitudinal velocity component on time (within one period) at three points of the cross-section: at $r/a = 0$ (on the axis), 0.5 and 0.9 (near the wall). The number N (16) was equal to unity. At a distance x equal to half of the shock formation length x_s, the nonlinear effects are expressed weakly and the profiles are similar to the harmonic ones. However, the diffraction influence is marked, and leads to phase shifts and to energy diffusion from the central part of beam to its borders. At a distance $x = x_s$ the shock has to be formed in the plane wave. However, the phase discrepancy of the harmonics slows down this process particularly in regions distant from the axis. Stable shock front formation takes place $(x/x_s = 7)$ just after the uniform distribution in cross section is reached for all wave characteristics, as result of diffusion and reflection from walls.

Let us discuss now the principal effect of nonlinear wave theory — the self-focusing of sawtooth wave beams. As distinct from the inertialess self-focusing in cubically nonlinear media described in Section 2.4, we deal here with thermal self-action in a quadratic nonlinear medium.

The thermal self-focusing of beams, well known in optics [33], comes about because of the dependence of the wave velocity on the temperature and because of the nonuniform heating of the medium by the beam. The thermal self-focusing of a harmonic wave, predicted in Ref. [143], has been observed in acoustic experiments in highly viscous liquids [144, 145]. The peculiar features of these experiments are connected with the breakdown of the

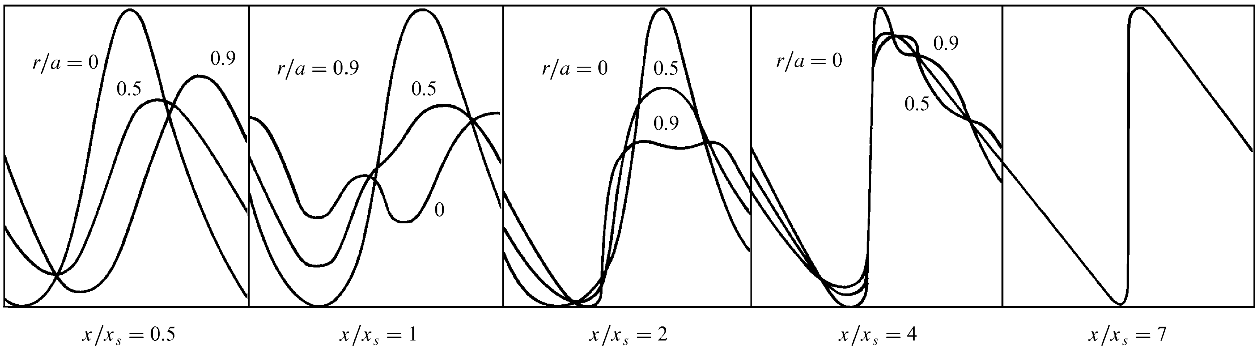

Figure 20. Profiles of one period of a wave for of cross section r/a of the tube equal to 0, 0.5 and 0.9 at different distances x.

thermal lens by the acoustic wind, with the complicated near-field structure of acoustic sources (where the concept of beam boundary is meaningless), as well as with the 'self-clearing' of a medium which is caused by the absorption decreasing as the temperature rises [26]. If these difficulties are minimised [147] the phenomenon will be similar to the self-action of laser beams in media with a large coefficient of sound absorption α; the effect disappears as $\alpha \to 0$. As distinct from the optical analogue, the thermal self-action of 'saws' takes place even in ideal media with $\alpha = 0$, because nonlinear absorption of wave energy occurs, and the medium is heated (see Section 6).

In Ref. [8] an experiment is described on the observation of self-focusing of the sawtooth wave. A beam with power 20 W, width 30 mm and frequency 2 MHz was radiated into water where the periodic 'saw' was formed during the propagation. Then the 'saw' penetrated to an acetone-filled cell. Acetone was used as the medium for thermal self-focusing investigation, because it has a small coefficient α and a negative temperature coefficient of sound velocity $\delta = c_0^{-1}(\partial c/\partial T)_p$, i.e. it is (in contrast to the water) the focusing medium. A marked increase of the intensity on the axis of the beam was observed.

The theory of this phenomenon is developed in Refs [7, 9]. The most simple model will be obtained if one can neglect the diffraction and describe the beam using a nonlinear geometric acoustics approximation:

$$\frac{\partial p}{\partial x} - \frac{\varepsilon}{c_0^3 \rho_0} p \frac{\partial p}{\partial \theta} - \frac{b}{2c_0^3 \rho_0} \frac{\partial^2 p}{\partial \theta^2} + \frac{\partial \psi}{\partial r} \frac{\partial p}{\partial r} + \frac{1}{2} p \Delta_\perp \psi = 0 \; , \quad (75)$$

$$\frac{\partial \psi}{\partial x} + \frac{1}{2}\left(\frac{\partial \psi}{\partial r}\right)^2 = -\delta T \; , \quad (76)$$

$$\frac{\partial T}{\partial t} - \frac{\chi}{\rho_0 c_p} \Delta_\perp T = \frac{b}{c_0^4 \rho_0^3 c_p} \overline{\left(\frac{\partial p}{\partial \theta}\right)^2} \; . \quad (77)$$

Eqn (75) differs from the Burgers' equation in the last two terms, which take into account the change in the inclination and in the cross section of the ray tubes; here $\theta = t - x/c_0 - \psi(x, r)/c_0$, ψ is the shift in the wave front because of heating of the medium. The eikonal Eqn (76) describes the bending of rays because of the increase in the temperature of the medium T. The right side of the heat conduction Eqn (77) is responsible for the transformation of acoustic energy into thermal energy; as in Eqn (49), it takes into consideration two kinds of losses: linear and nonlinear ones.

In considering a sawtooth wave, each period of which can be described by the Khokhlov solution

$$p = A(x, r)\left[-\frac{\omega\theta}{\pi} + \tanh\left(\frac{\varepsilon}{b} A\theta\right)\right], \qquad -\pi < \omega\theta < \pi \; ,$$

it is possible to eliminate the 'fast time' θ and pass from the field variable $p(x, r, \theta)$ to the peak pressure $A(x, r)$. Eqns (75), (77) take the form

$$\frac{\partial A}{\partial x} + \frac{\partial \psi}{\partial r}\frac{\partial A}{\partial r} + \frac{1}{2} A \Delta_\perp \psi = -\frac{\varepsilon\omega}{\pi c_0^3 \rho_0} A^2 \; , \quad (78)$$

$$\frac{\partial T}{\partial t} - \frac{\chi}{\rho_0 c_p} \Delta_\perp T = \frac{2}{3\pi} \frac{\varepsilon\omega}{c_0^4 \rho_0^3 c_p} A^3 \; . \quad (79)$$

The resultant set of Eqns (78), (79) and (76) describes the thermal self-action of sawtooth wave beams. It is seen from Eqn (78) that the absorption is purely nonlinear; in the linear case, in place of the right side we would have the term $-\alpha A$. The right-hand side of Eqn (79) is also connected with this feature: the heat release power is $\sim A^3$ (in the linear case it would be proportional to A^2).

The results of the solution of this system can describe the following processes. At the beginning the beam expands with increase in the distance because of isotropisation (see Section 3), but the peak pressure decreases because of nonlinear absorption. With the passage of time, the medium heats up, and the strength of the thermal lens increases. Self-focusing of the beam occurs, and the focus moves toward the source. At $t \to \infty$ the steady-state regime will be established; as this takes place, there exists a distance between the source and the nonlinear focus where the beam width has a maximum, but the peak pressure has a minimum value.

An interesting phenomenon can be observed for the focusing of the beam into a self-defocusing medium ($\delta > 0$), the most important example of which is water at room temperatures. The thermal self-action in this case hinders the focusing and, as a result, nonlinear constriction of finite dimensions does appear there [9]. For example, let the beam of sawtooth waves in water have the following parameters: initial radius of 3 cm, curvature radius of the initial wave front 9.4 cm, peak pressure 1.3 atm and fundamental frequency 4 MHz. The constriction radius is equal to 3.6 mm in this case, while in the absence of self-action and with account of diffraction, it would be 0.36 mm. So, the self-defocusing broadens the constriction by an order. This phenomenon does not require extreme values of the wave amplitude; it appears to have been observed many times during operation with medical instruments (used for the imaging of internal structure of tissues, for ultrasonic therapy and hyperthermy [148]).

9. Conclusions

An attempt was made in this review to describe only some of the phenomena connected with the propagation of sawtooth-shaped disturbances, which are interesting (because of their specificity) for nonlinear wave physics. The problems of giving complete information about these waves seemed to be intractable from the beginning, because almost all the questions mentioned here (state-of-the-art of the sonic boom problem, shock wave lithotripsy, creation of extremely strong fields at the focus, nonlinear diagnostics, propagation of shocked waves through media with complicated internal dynamics and structure, and many others) merit individual generalisation. It would be well to consider the mathematical model describing the sawtooth waves in more detail as well as the asymptotic and numerical methods of solution of corresponding nonlinear equations. Perhaps it will be done later.

Acknowledgements. I am grateful to I A Yakovlev for his suggestion to write this review.

The work is supported partly by the Russian Foundation of Fundamental Research (project 93-02-15453), by the Centre for Fundamental Natural Sciences and by the Soros Foundation.

References

1. Rudenko O V, Soluyan S I *Teoreticheskie Osnovy Nelineinoi Akustiki* (Moscow: Nauka, 1975);
Rudenko O V, Soluyan S I *Theoretical Foundations of Nonlinear Acoustics* (New York: Plenum, Consultants Bureau, 1977)
2. Burov V A, Krasil'nikov V A *Dokl. Akad. Nauk SSSR* **118** (5) 920 (1958) [*Sov. Phys. Dokl.* (3) 173 (1959)]
3. Zarembo L K, Krasil'nikov V A, Shklovskaya-Kordi V V *Dokl. Akad. Nauk SSSR* **109** (4) 731 (1956) [*Sov. Phys. Dokl.* **1** 434 (1957)]
4. Zarembo L K, Krasil'nikov V A *Vvedenie v Nelineinuyu Akustiku* (Introduction to Nonlinear Acoustics) (Moscow: Nauka, 1966)
5. Naugol'nykh K A, in *Moshchnye Ultrazvukovye Polya* (High-Power Ultrasonic Fields) (Moscow: Nauka, 1967) p. 7
6. Beyer R T *Nonlinear Acoustics* (USA: Naval Sea Systems Command, 1974)
7. Rudenko O V, Sapozhnikov O A *Vestn. Mosk. Univ. Fiz. Astron.* **29** (6) 91 (1988) [*Mosc. Univ. Phys. Bull.* **43** (6) 106 (1989)]
8. Karabutov A A, Rudenko O V, Sapozhnikov O A *Akust. Zh.* **35** (1) (67) (1989) [*Sov. Phys. Acoust.* **35** (1) 40 (1989)]
9. Rudenko O V, Sagatov M M, Sapozhnikov O A *Zh. Eksp. Teor. Fiz.* **96** (3 (9)) 808 (1990) [*Sov. Phys. JETP* **71** (3) 449 (1990)]
10. Karabutov A A, Rudenko O V, Sapozhnikov O A *Akust. Zh.* **34** (4) 644 (1988) [*Sov. Phys. Acoust.* **34** (4) 371 (1988)]
11. Rudenko O V, in *Advances in Nonlinear Acoustics* (Singapore: World Scientific, 1993) p. 3
12. Rudenko O V, Sapozhnikov O A *Kvantovaya Elektron. Mosk.* **29** (10) 1028 (1993) [*Quantum Electron.* **23** 896 (1993)]
13. Rudenko O V, Sapozhnikov O A *Zh. Eksp. Teor. Fiz.* **106** (2(8)) 395 (1994) [*J. Exp. Theor. Phys.* **79** (2) 220 (1994)]
14. Musatov A G, Rudenko O V, Sapozhnikov O A *Akust. Zh.* **38** (3) 502 (1992) [*Sov. Phys. Acoust.* **38** (3) 274 (1992)]
15. Musatov A G, Sapozhnikov O A *Akust. Zh.* **39** (3) 510 (1993) [*Acoust. Phys.* **39** (2) 166 (1993)]
16. Rudenko O V, Sapozhnikov O A, in *Proceedings of IEEE 1992 Ultrasonics Symposium* Vol. 1 (New York: IEEE, 1992) p. 489
17. Rudenko O V *Defektoskopiya* (8) 24 (1993)
18. Rudenko O V, Sapozhnikov O A *Vestn. Mosk. Univ. 3, Fiz. Astron.* **32** (1) 3 (1991) [*Mosc. Univ. Phys. Bull.* **46** (1) 5 (1991)]
19. Andreev V G, Veroman V Yu, Denisov G A, Rudenko O V, Sapozhnikov O A *Akust. Zh.* **38** (4) 588 (1992) [*Sov. Phys. Acoust.* **38** (4) 325 (1992)]
20. Rudenko O V *Usp. Fiz. Nauk* **149** (3) 413 (1986) [*Sov. Phys. Usp.* **29** (7) 620 (1986)]
21. Rudenko O V, Sukhorukova A K, Sukhorukov A P *Akust. Fiz.* **40** (2) 290 (1994) [*Acoust. Phys.* **40** (2) 264 (1994)]
22. Maglieri D J *J. Acoust. Soc. Am.* **92** (4) 2328 (1992)
23. Pierse A D, in *Advances in Nonlinear Acoustics* (Singapore: World Scientific, 1993) p. 7
24. Akhmanov S A, Khokhlov R V *Osnovy Nelineinoi Optiki* (Foundations of Nonlinear Optics) (Moscow: VINITI, 1964)
25. Akhmanov S A, Vysloukh V A, Chirkin A S *Optika Femtosekundnykh Lazernykh Impul'sov* (Optics of Femtosecond Laser Pulses) (Moscow: Nauka, 1988)
26. Bunkin F V, Kravtsov Yu A, Lyakhov G A *Usp. Fiz. Nauk* **149** (3) 391 (1986) [*Sov. Phys. Usp.* **29** (7) 607 (1986)]
27. Blackstock D T *J. Acoust. Soc. Am.* **39** (4) 1019 (1966)
28. Lyakhov G A, Rudenko O V *Akust. Zh.* **20** (5) 738 (1974) [*Sov. Phys. Acoust.* **20** 447 (1975)]
29. Novikov B K, Rudenko O V *Akust. Zh.* **22** (3) 461 (1976) [*Sov. Phys. Acoust.* **22** (3) 258 (1976)]
30. Landauer R *J. Appl. Phys.* **31** (3) 479 (1960)
31. Vasil'eva O A, Karabutov A A, Lapshin E A, Rudenko O V *Vzaimodeistvie Odnomernykh Voln v Sredakh bez Dispersii* (Interaction of One-Dimensional Waves in Media without Dispersion) (Moscow: Moscow University Press, 1983)
32. Gurbatov S N, Malakhov A N *Akust. Zh.* **25** (1) 53 (1979) [*Sov. Phys. Acoust.* **25** (1) 28 (1979)]
33. Akhmanov S A, Sukhorukov A P, Khokhlov R V *Usp. Fiz. Nauk* **93** (1) 19 (1967) [*Sov. Phys. Usp.* **10** (1) 609 (1967)]
34. Bespalov V I, Talanov V I *Pis'ma Zh. Eksp. Teor. Fiz.* **3** (12) 471 (1966) [*JETP Lett.* **3** 307 (1966)]
35. Lee-Bapty J P, Crighton D G *Philos. Trans. R. Soc. London A* **323** 173 (1987)
36. Webster D A, Theobald M A, Blackstock D T, in *Proceedings of the 9th International Congress on Acoustics, Madrid* **2** (32) 740 (1977)
37. Andreev V G, Karabutov A A, Rudenko O V *Akust. Zh.* **31** (4) 423 (1985) [*Sov. Phys. Acoust.* **31** (4) 252 (1985)]
38. Webster D A, Blackstock D T *J. Acoust. Soc. Am.* **62** (3) 518 (1977)
39. Rudenko O V, Soluyan S I, Khokhlov R V *Akust. Zh.* **19** (6) 871 (1973) [*Sov. Phys. Acoust.* **19** 556 (1974)]
40. Ostrovskii L A, Fridman V E *Akust. Zh.* **18** (4) 584 (1972)[*Sov. Phys. Acoust.* **18** (4) 478 (1973)]
41. Bakhvalov N S, Zhileikin Ya M, Zabolotskaya E A *Nelineinaya Teoriya Zvukovykh Puchkov* (Moscow: Nauka, 1982);
Bakhvalov N S, Zhileikin Ya M, Zabolotskaya E A *Nonlinear Theory of Sound Beams* (New York: American Institute of Physics, 1987)
42. Khokhlov R V *Radiotekh. Elektron.* **6** (6) 917 (1961)
43. Zabolotskaya E A, Khokhlov R V *Akust. Zh.* **15** (1) 40 (1969) [*Sov. Phys. Acoust.* **15** 35 (1969)]
44. Kuznetsov V P *Akust. Zh.* **16** (4) 548 (1970) [*Sov. Phys. Acoust.* **16** (4) 475 (1970)]
45. Kadomtsev B B, Petviashvili V I *Dokl. Akad. Nauk SSSR* **192** (4) 753 (1970) [*Sov. Phys. Dokl.* **15** (6) 539 (1970)]
46. Rudenko O V, Soluyan S I, Khokhlov R V *Akust. Zh.* **20** (3) 449 (1974) [*Sov. Phys. Acoust.* **20** (3) 271 (1974)]
47. Andreev V G, Rudenko O V, Sapozhnikov O A, Khokhlova V A *Vestn. Mosk. Univ. Fiz. Astron.* **26** (3) 58 (1985) [*Mosc. Univ. Phys. Bull.* **40** (3) 67 (1985)]
48. Vinogradova M B, Rudenko O V, Sukhorukov A P *Teoriya Voln* (Theory of Waves) (2nd edition) (Moscow: Nauka, 1990)

49. Hobaek H *Parametric Acoustic Transmitting Arrays—a Survey of Theories and Experiment* Sci. Techn. Report 99 (Norway: University of Bergen, 1977)
50. Hamilton M F, Tjotta J N, Tjotta S *J. Acoust. Soc. Am.* **78** (1) 202 (1985)
51. Aanonsen S I, Barkve T, Tjotta J N, Tjotta S *J. Acoust. Soc. Am.* **75** (3) 749 (1984)
52. Novikov B K, Rudenko O V, Timoshenko V I *Nelineinaya Gidroakustica* (Leningrad: Sudostroenie, 1981); Novikov B K, Rudenko O V, Timoshenko V I *Nonlinear Underwater Acoustics* (New York: Amererican Institute of Physics, 1987)
53. Rudenko O V, Soluyan S I, Khokhlov R V *Dokl. Akad. Nauk SSSR* **225** (5) 1053 (1975) [*Sov. Phys. Dokl.* **20** 836 (1975)]
54. Courant R, Hilbert D *Methods of Mathematical Physics* (New York: Interscience, 1953)
55. Bakhvalov N S, Zhileikin Ya M, Zabolotskaya E A, Khokhlov R V *Akust. Zh.* **22** (4) 487 (1976) [*Sov. Phys. Acoust.* **22** (4) 272 (1976)]
56. Hamilton M F, Khokhlova V A, Rudenko O V *J. Acoust. Soc. Am.* **96** (5) 3321 (1994)
57. Lapidus Yu R, Rudenko O V *Akust. Zh.* **30** (6) 797 (1984) [*Sov. Phys. Acoust.* **30** (6) 473 (1984)]
58. Lapidus Yu R, Soluyan S I *Akust. Zh.* **31** (5) 615 (1985) [*Sov. Phys. Acoust.* **31** (5) 368 (1985)]
59. Ginsberg J H *J. Acoust. Soc. Am.* **76** (4) 1201 (1984)
60. Coulouvrat F Y *J. Acoust. Soc. Am.* **90** (3) 1592 (1991)
61. Bacon D R, Baker A C *Phys. Med. Biol.* **34** 1633 (1989)
62. Baker A C, Anastasiadis K, Humphrey V F *J. Acoust. Soc. Am.* **84** (5) 1483 (1988)
63. Landau L D, Lifshitz E M *Gidrodinamika* (Moscow: Nauka, 1976); Landau L D, Lifshitz E M *Fluid Mechanics* (New York: Pergamon Press, 1984)
64. Lin C C, Reissner E, Tsien H S *J. Math. Phys.* **27** 3 (1948)
65. Karabutov A A, Rudenko O V *Dokl. Akad. Nauk SSSR* **248** (5) 1082 (1979)
66. Cramer M S, Seebass A R *J. Fluid Mech.* **88** (2) 209 (1978)
67. Spektor M D *Pis'ma Zh. Eksp. Teor. Fiz.* **35** (5)181 (1982) [*JETP Lett.* **35** (5) 221 (1982)]
68. Munin A G, Kvitka V E *Aviatsionnaya Akustika* (Aviational Acoustics) (Moscow: Mashinostroenie, 1973)
69. Pierce A D, Maglieri D J *J. Acoust. Soc. Am.* **51** (3) 702 (1972)
70. Fridman V E Abstract of Doctorate Thesis in Physicomathematical Sciences (Moscow: General Physics Institute, 1985)
71. Whitham G B *Linear and Nonlinear Waves* (New York: Wiley Interscience, 1974)
72. Pelinovskii E N, Fridman V E, Engel'brekht Yu K *Nelineinye Evolyutsionnye Uravneniya* (Nonlinear Evolution Equations) (Tallin: Valgus, 1984)
73. Naygol'nykh K A, Ostrovskii L A *Nelineinye Volnovye Protsessy v Akustike* (Nonlinear Wave Processes in Acoustics) (Moscow: Nauka, 1990)
74. Blokhintsev D I *Akustika Neodnorodnoi Dvizhushcheisya Sredy* (Acoustics of an Inhomogeneous Moving Medium) (2nd edition) (Moscow: Nauka, 1981)
75. Kravtsov Yu A, Orlov Yu I *Geometricheskaya Optika Neodnorodnykh Sred* (Geometric Optics of Inhomogeneous Media) (Moscow: Nauka, 1980)
76. Ostashev V E *Rasprostranenie Zvuka v Dvizhushchikhsya Sredakh* (Sound Propagation in Moving Media) (Moscow: Nauka, 1992)
77. Gubkin K E *Prikl. Mat. Mekh.* **22** (4) 561 (1958)
78. Ryzhov O S *Zh. Prikl. Mekh. Tekh. Fiz.* (2) 15 (1961)
79. Zhilin Yu L *Tr. TsAGI* 1489 3 (1973)
80. Zarembo L K, Chunchuzov I A *Akust. Zh.* **23** (1) 143 (1977) [*Sov. Phys. Acoust.* **23** (1) 78 (1977)]
81. Pelinovskii E N, Soustova I A, Fridman V E *Akust. Zh.* **24** (5) 740 (1978) [*Sov. Phys. Acoust.* **24** (5) 415 (1978)]
82. Reiso E, Tjotta J N, Tjotta S, in *Frontiers of Nonlinear Acoustics* (London: Elsevier, 1990) p. 177
83. Rudenko O V, Sukhorukova A K, Sukhorukov A P *Akust. Zh.* **41** (2) 291 (1995) [*Acoust. Phys.* **41** (2) 251 (1995)]
84. Musatov A G, Sapozhnikov O A *Vestn. Mosk. Univ. 3, Fiz. Astron.* **34** (4) 94 (1993) [*Mosc. Univ. Phys. Bull.* **48** (4) 88 (1993)]
85. Nauygol'nykh K A, Soluyan S I, Khokhlov R V *Akust. Zh.* **9** (1) 54 (1963) [*Sov. Phys. Acoust.* **9** 42 (1963)]
86. Sutin A M, in *Nelineinaya Akustika* (Nonlinear Acoustics) (Gor'kii: Applied Physics Institute, 1980) p. 45
87. Ostrovskii L A, Sutin A M *Dokl. Akad. Nauk SSSR* **221** (6) 1300 (1975) [*Sov. Phys. Dokl.* **20** 275 (1975)]
88. Smith C W, Beyer R T *J. Acoust. Soc. Am.* **46** (3) 806 (1969)
89. Borisov Yu Ya, Gynkina N M *Akust. Zh.* **19** (4) 616 (1973) [*Sov. Phys. Acoust.* **19** 389 (1974)]
90. Cathignol D, Chapelon J Y, in *Advances in Nonlinear Acoustics* (Singapore: World Scientific, 1993) p. 21
91. Delius M, in *Frontiers of Nonlinear Acoustics* (London: Elsevier, 1990) p. 31
92. Church C C, Crum L A, in *Proceedings of the 13th International Congress on Acoustics, Belgrade, 1989* Vol. 4, p. 205
93. Agarval L, Singh V R, Sud S P, in *Proceedings of the 14th International Congress on Acoustics, Beijing, 1992* Vol. 2, p. 1
94. Takayama K, in *Proceedings of 15 International Workshop on Shock Wave Focusing, Sendai, Japan, 1989* p. 217
95. Rudenko O V, Veroman V Yu, Denisov G A et al. *Optoakusticheskii Izluchatel' dlya Beskontaktnogo Razrusheniya Konkrementov v Tele Bioob''ekta* (Optoacoustic Radiator for Contactless Destruction of Calculi in the Body of a Biological Object) Patent (author's certificate No. 1673085)
96. Gusev V E, Karabutov A A *Lazernaya Optoakustika* (Laser Optoacoustics) (Moscow: Nauka, 1991)
97. Akhmanov S A, Gordienko V M, Karabutov A A et al, in *IX Vsesoyuzn. Akust. Konf.* (All-Union Acoustics Conference) (Moscow: Acoustics Institute, 1977) 4 IV-6, p. 25
98. Bozhkov A I, Bunkin F V, Galstyan A M et al. *Izv. Akad. Nauk SSSR Ser. Fiz.* **46** (8) 1624 (1982) [*Bull. Acad. Sci. USSR, Phys. Ser.* **46** (8) 168 (1982)]
99. Askar'yan G A, Klebanov L D *Kvantovaya Electron. Mosk.* **15** (11) 2167 (1988) [*Sov. J. Quantum Electron.* **18** (11) 1359 (1988)]
100. Musatov A G, Rudenko O V, Sapozhnikov O A, in *Advances in Nonlinear Acoustics* (Singapore: World Scientific, 1993) p. 321
101. Coleman A J, Saunders J E, Preston R C, Bacon D R *Ultrasound Med. Biol.* **13** 651 (1987)
102. Coleman A J, Saunders J E *Ultrasound Med. Biol.* **15** 213 (1989)
103. Muller M, in *Proceedings of the 13th International Congress on Acoustics, Belgrade, 1989* Vol. 1, p. 259
104. Musatov A G, Sapozhnikov O A *Akust. Zh.* **39** (2) 315 (1993) [*Acoust. Phys.* **39** (2) 166 (1993)]
105. Sapozhnikov O A *Akust. Zh.* **37** (4) 760 (1991) [*Sov. Phys. Acoust.* **37** (4) 395 (1991)]
106. Zhileikin Ya M, Rudenko O V *Akust. Zh.* **27** (3) 363 (1981) [*Sov. Phys. Acoust.* **27** (3) 200 (1981)]
107. Zhileikin Ya M, Osipik Yu I, in *Sovremennye Problemy Matematicheskogo Modelirovaniya* (Modern Problems of Mathematical Modelling) (Moscow: Moscow University Press, 1984) p. 152
108. Rudenko O V *Pis'ma Zh. Eksp. Teor. Fiz.* **20** (7) 445 (1974) [*JETP Lett.* **20** (7) 203 (1974)]
109. Karabutov A A, Lapshin E A, Rudenko O V *Zh. Eksp. Teor. Fiz.* **71** (1 (7)) 111 (1976) [*Sov. Phys. JETP* **44** (1) 58 (1976)]
110. Rudenko O V *Akust. Zh.* **29** (3) 398 (1983) [*Sov. Phys. Acoust.* **29** (3) 234 (1983)]
111. Andreev V G, Rudenko O V, in *Tr. 10 Vsesoyuzn. Akust. Konf.* (Proceedings of the 10th All-Union Acoustics Conference) (Moscow: Acoustics Institute, 1983) section B, p. 24
112. Andreev V G, Gusev V E, Karabutov A A, Rudenko O V, Sapozhnikov O A *Akust. Zh.* **31** (2) 275 (1985) [*Sov. Phys. Acoust.* **31** (2) 162 (1985)]
113. Gurbatov S N, Rudenko O V *Nelineinaya Akustika v Zadachakh* (Nonlinear Acoustics in Problems) (Moscow: Moscow University Press, 1990)

114. Zakharov V E, Sagdeev R Z *Dokl. Akad. Nauk SSSR* **192** (2) 297 (1970) [*Sov. Phys. Dokl.* **15** 439 (1970)]
115. Kadomtsev B B, Petviashvili V I *Dokl. Akad. Nauk SSSR* **208** (4) 794 (1973) [*Sov. Phys. Dokl.* **18** (1973)]
116. Naugol'nykh K A, Rybak S A *Zh. Eksp. Teor. Fiz.* **68** (1) 78 (1975) [*Sov. Phys. JETP* **41** 39 (1975)]
117. Rudenko O V, Khokhlova V A *Akust. Zh.* **34** (3) 500 (1988) [*Sov. Phys. Acoust.* **34** (3) 289 (1988)]
118. Rudenko O V, Khokhlova V A *Akust. Zh.* **37** (1) 182 (1991) [*Sov. Phys. Acoust.* **37** (1) 90 (1991)]
119. Gurbatov S N, Saichev A I *Zh. Eksp. Teor. Fiz.* **80** (2) 689 (1981) [*Sov. Phys. JETP* **53** 347 (1981)]
120. Gurbatov S N, Malakhov A N, Saichev A I *Nelineinye Sluchainye Volny v Sredakh bez Dispersii* (Moscow: Nauka, 1990);
Gurbatov C N, Malakhov A N, Saichev A I *Nonlinear Random Waves and Turbulence in Nondispersive Media: Waves, Rays and Particles* (Manchester: Manchester University Press, 1991)
121. Lapshin E A et al. *Application Package NACSI* (*1-1.2: Plane, Converging and Diverging Waves in Dissipative and Relaxing Media; 2.1-4: High-intensity Acoustic Beams in Nonlinear Media*) (Moscow: Dialogue–MGU, 1992)
122. Khokhlova V A, Sapozhnikov O A *J. Acoust. Soc. Am.* **96** (5) 3321 (1994)
123. Gurbatov S N, Saichev A I, Yakushkin I G *Usp. Fiz. Nauk* **141** (2) 221 (1983) [*Sov. Phys. Usp.* **26** 857 (1983)]
124. Moffett M B, Konrad W L, Carlton L F *J. Acoust. Soc. Am.* **63** (4) 1048 (1978)
125. Burov V A, Krasil'nikov V A, Tagunov E Ya *Vestn. Mosk. Univ. 3, Fiz. Astron.* **19** (4) 53 (1978) [*Mosc. Univ. Phys. Bull.* **33** (4) 60 (1978)]
126. Volyak K I, Gorshkov A S, Rudenko O V *Vestn. Mosk. Univ. 3, Fiz. Astron.* **16** (1) 32 (1975) [*Mosc. Univ. Phys. Bull.* **30** (1) 40 (1975)]
127. Makarov S N *Acustica* **80** (1) 1 (1994)
128. Morfey C L, in *Advances in Nonlinear Acoustics* (Singapore: World Scientific, 1993) p. 167
129. Westervelt P J *J. Acoust. Soc. Am.* **96** (5) 3320 (1994)
130. Kaner V V, Rudenko O V, Khokhlov R V *Akust. Zh.* **23** (5) 756 (1977) [*Sov. Phys. Acoust.* **23** (5) 432 (1977)]
131. Seymour B R, Mortell M P *J. Fluid Mech.* **52** (2) 353 (1973)
132. Temkin S *J. Acoust. Soc. Am.* **45** (1) 224 (1969)
133. Ostrovskii L A *Akust. Zh.* **20** (1) 140 (1974) [*Sov. Phys. Acoust.* **20** (1) 88 (1974)]
134. Ochmann M *J. Acoust. Soc. Am.* **77** (1) 61 (1985)
135. Gusev V E *Akust. Zh.* **30** (2) 204 (1984) [*Sov. Phys. Acoust.* **30** (2) 121 (1984)]
136. Kaner V V, Rudenko O V *Vestn. Mosk. Univ. 3, Fiz. Astron.* **19** (4) 78 (1978) [*Mosc. Univ. Phys. Bull.* **33** (4) 63 (1978)]
137. Nayfeh A H, Kaiser J E, Telionis D P *AIAA J.* **13** (2) 130 (1975)
138. Webster D A, Blackstock D T *J. Acoust. Soc. Am.* **63** (3) 687 (1978)
139. Smith R T, Bjorno L, Stephens R W B *Acustica* **39** (2) 123 (1978)
140. Hamilton M F, Ten Cate J A *J. Acoust. Soc. Am.* **84** (1) 327 (1988)
141. Nakamura A *Mem. Inst. Sci. Ind. Res., Osaka Univ.* **32** 23 (1975)
142. Zhileikin Ya M, Zhuravleva T M, Rudenko O V *Akust. Zh.* **26** (1) 62 (1980) [*Sov. Phys. Acoust.* **26** (1) 32 (1980)]
143. Askar'yan G A *Pis'ma Zh. Eksp. Teor. Fiz.* **4** (4) 144 (1966) [*JETP Lett.* **4** (4) 99 (1966)]
144. Assman V A, Bunkin F V, Vernik A V et al. *Pis'ma Zh. Eksp. Teor. Fiz.* **41** (4) 148 (1985) [*JETP Lett.* **41** (4) 182 (1985)]
145. Andreev V G, Karabutov A A, Rudenko O V, Sapozhnikov O A *Pis'ma Zh. Eksp. Teor. Fiz.* **41** (9) 381 (1985) [*JETP Lett.* **41** (9) 466 (1985)]
146. Karabutov A A, Rudenko O V, Sapozhnikov O A *Vestn. Mosk. Univ. 3, Fiz. Astron.* **29** (4) 63 (1988) [*Mosc. Univ. Phys. Bull.* **43** (4) 68 (1988)]
147. Armeev V Yu, Karabutov A A, Sapozhnikov O A *Akust. Zh.* **33** (2) 177 (1987) [*Sov. Phys. Acoust.* **33** (2) 109 (1987)]
148. *Primenenie Ultrazvuka v Meditsine* (Application of Ultrasound in Medicine) (Transl. from Engl., eds L R Gavrilov, A P Sarvazyan) (Moscow: Mir, 1989);
Physical Principles of Medical Ultrasonics (Ed. C R Hill) (New York: Harwood Ltd, 1986)